The excitation spectrum and the Bose condensate in liquid ^{4}He

Zh. A. Kozlov
Joint Institute for Nuclear Research, Dubna

Fiz. Élem. Chastits At. Yadra **27**, 1705–1751 (November–December 1996)

A review is given of studies of liquid ^{4}He by inelastic scattering of neutrons on the basis of results obtained at the reactors IBR-30 and IBR-2. Attention is focused on the structure of the excitation spectra in both the normal and superfluid phases, and also on the search for the Bose condensate and its investigation. © *1996 American Institute of Physics.*
[S1063-7796(96)00406-8]

INTRODUCTION

The liquid formed of ^{4}He atoms possesses a number of unique properties. Kapitza[1] found that liquid ^{4}He becomes a superfluid at temperatures below $T_\lambda = 2.17$ K. Landau[2] showed that the superfluidity follows from the shape of the spectrum of elementary excitations of the Bose liquid and can occur when the flow rate of the liquid is smaller than the critical value determined from the excitation spectrum. London[3] treated liquid ^{4}He as an ideal Bose gas and suggested that the superfluidity of ^{4}He is related to the phenomenon of Bose–Einstein condensation, i.e., to the presence of a macroscopic number of ^{4}He atoms in the ground state with momentum $p=0$. The phenomenon of condensation in momentum space was first pointed out in 1925 by Einstein. Bogolyubov[4] showed that the Bose condensation is preserved for a weakly nonideal Bose gas, and that the structure of the energy levels satisfies the Landau superfluidity conditions. The influence of the Bose condensate on the shape of the spectrum has been investigated in many theoretical studies, begun by Bogolyubov and Belyaev.[5] The development of these ideas led to the conclusion that the excitation spectrum of superfluid ^{4}He has a complicated structure.

Neutron studies of liquid ^{4}He take advantage of the possibility of studying both the collective and the individual motions of atoms. It is therefore interesting to use neutrons to study the *excitation spectrum* in the superfluid and normal phases of liquid ^{4}He, and also to study the phenomenon of *Bose condensation*. By combining the results of neutron investigations with the large amount of information obtained by studying the *superfluidity* of ^{4}He, it is possible to establish correlations between the phenomena of superfluidity and Bose condensation. A special role in these correlations is played by the excitation spectrum, the shape of which, on the one hand, determines the condition for Landau superfluidity and, on the other, is associated with the presence of the Bose condensate.

In 1961, Henshaw and Woods[6] used the method of neutron inelastic scattering to measure the dispersion curve of the excitations in superfluid ^{4}He, which coincided with the Landau prediction for the shape. Later on, neutron studies of ^{4}He improved the parameters of the dispersion curve as a function of temperature and pressure at various values of the wave vector q (Refs. 7–10). In Fig. 1 we show the dispersion curve from Ref. 7, where we have indicated the phonon, maxon, and roton regions. The two-component nature of the spectrum of neutrons inelastically scattered on superfluid ^{4}He in the maxon–roton region was pointed out in 1978 by Woods and Svensson.[11] They essentially assumed that the neutrons are scattered by the normal and superfluid components independently and in different ways. Naturally, attempts were made to find a theoretical justification of the results of this experiment. However, they were unsuccessful.

In parallel with the study of the excitation spectrum, work was done to seek and study the Bose condensate in liquid ^{4}He at large energy transfers $\varepsilon \gg \Delta$ and wave-vector transfers $q \gg q_r$, where Δ and q_r are the roton energy and wave vector. It was assumed that high-energy neutrons scatter on ^{4}He atoms as on quasifree particles, and in this case it is possible to separate the spectrum of neutrons scattered on the atoms of the Bose condensate from the rest of the spectrum because the atoms of the Bose condensate do not produce Doppler broadening. However, it was not possible to distinguish the spectra visually, and therefore various methods were used to analyze the spectra of single-atom neutron scattering. These allowed the relative density of the Bose condensate to be estimated. To make the results more reliable, this analysis was usually performed at various temperatures or pressures.

Fundamental data on the liquid dynamics can be obtained by measuring the doubly differential cross sections for neutron scattering. These are used to describe the liquid by means of a dynamical structure factor or, as it is commonly called, the scattering law $S(q,\omega)$ proposed by Van Hove.[12] The dynamical structure factor $S(q,\omega)$ is related to the doubly differential neutron scattering cross section as

$$\frac{d^2\sigma}{d\Omega dE} = \frac{b^2}{2\pi\hbar} \cdot \frac{k}{k_0} S(q,\omega),$$

where k_0 and k are the wave vectors of the incident and scattered neutrons, and b is the coherent scattering length. The transfers of wave vector q and energy ε in neutron scattering are

$$\mathbf{q} = \mathbf{k}_0 - \mathbf{k},$$

$$\varepsilon = \hbar\omega = E_0 - E,$$

where E_0 and E are the initial and final neutron energies.

This review is devoted to the study of liquid ^{4}He by the method of neutron inelastic scattering on the basis of the results obtained at the IBR-30 and IBR-2 reactors. Special attention is paid to the structure of the excitation spectra in

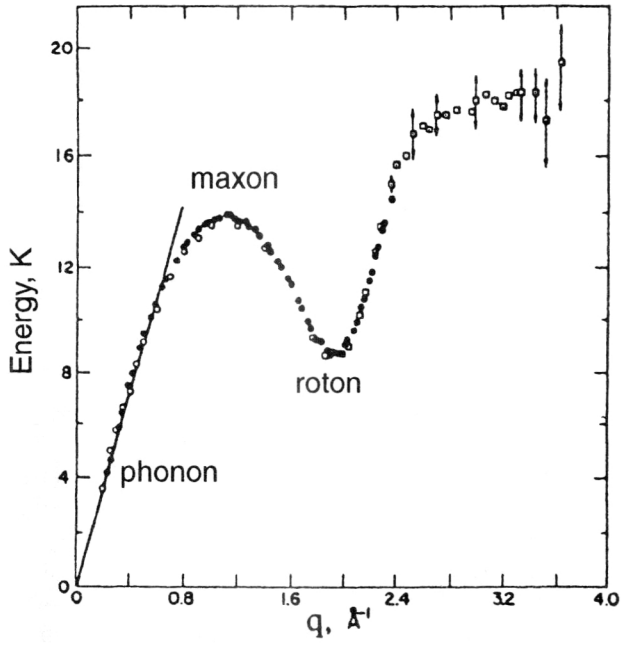

FIG. 1. Dispersion curve of superfluid ^{4}He at temperature 1.1 K (Ref. 7).

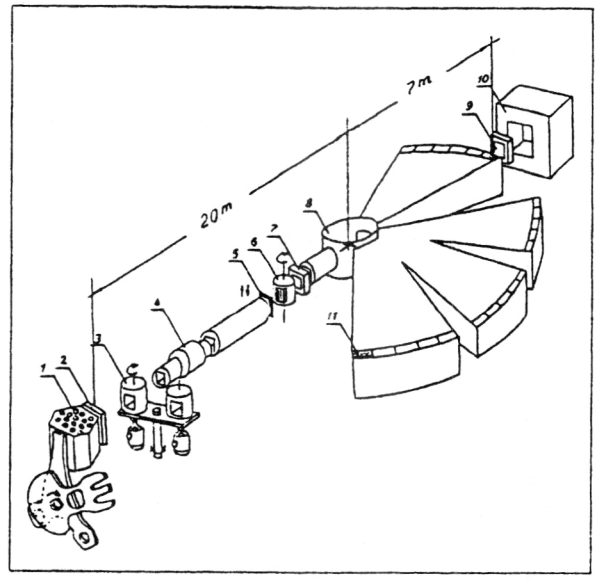

FIG. 2. Schematic diagram of the DIN-2PI spectrometer: (1) active zone of the IBR-2 reactor; (2) moderator; (3) chopper for background suppression; (4) collimator; (5) cadmium shutter; (6) selector–monochromator; (7) monitor 1; (8) sample chamber; (9) monitor 2; (10) catcher; (11) ^{3}He counters.

both the normal and the superfluid phases, to the search for and study of the Bose condensate, and to the discovery of correlations between the phenomena of superfluidity and Bose condensation.

1. THE EXPERIMENTAL INSTALLATION. THE MEASUREMENT TECHNIQUE

1.1. The setup

The experiments on neutron inelastic scattering on liquid ^{4}He at the Joint Institute for Nuclear Research in Dubna were performed with two spectrometers: first the DIN-1M (Refs. 13 and 14) at the IBR-30 reactor, and later the DIN-2PI (Ref. 15) at the IBR-2 reactor. Some of the measurements at wave vectors $q>7$ Å^{-1} were carried out in the booster operating mode of the IBR-30, which allowed a 1.5 to 2-fold increase of the energy resolution, owing to shortening of the duration of the reactor pulse and decrease of the neutron lifetime in the moderator. The two spectrometers are essentially identical and are based on the so-called "direct geometry," although there are of course differences in their construction and basic characteristics. These spectrometers are described in Ref. 15. In Fig. 2 we show a schematic picture of the arrangement of the main components of the DIN-2PI spectrometer. The detector systems of the spectrometers allowed simultaneous measurement of the scattered-neutron intensity in a wide range of scattering angles; for example, at the DIN-2PI, $\theta\approx(3-135)°$. Cryostats were used in the measurements,[16] allowing work with the sample of liquid ^{4}He at temperatures of from 4.2 to 0.42 K. The temperature was held fixed with an accuracy of ± 0.01 K.

1.2. The time-of-flight technique

The *time-of-flight technique* was used at the two spectrometers to measure the neutron inelastic scattering spectra. The monochromatic neutron beam incident on the sample was formed from a reactor pulse by a mechanical chopper, using the technique based on the time for the neutrons to traverse the first baseline. The energy of the neutrons scattered on the sample by an angle θ was determined from the time to traverse the second baseline between the sample and the detector.

The experimental spectra of the scattered neutrons in the region of one-particle excitations were analyzed in terms of energy. For this, the experimentally measured intensity as a function of scattering angle θ and neutron time of flight t was transformed into the dynamical structure factor $S(q,\varepsilon)$:

$$S(q,\varepsilon)=(2\pi\hbar/b^2)(E_0^2/E^2)d^2J(\theta,t)/d\Omega dt, \qquad (1.1)$$

where J is the count in the time channel.

The experimental spectra were measured for $\theta=$const, so that the transfers of wave vector q and energy ε are determined from the kinematic relation

$$q=0.695[2E_0\mp\varepsilon-2\cos\theta\sqrt{E_0(E_0\mp\varepsilon)}]^{1/2}, \qquad (1.2)$$

where the upper signs refer to neutron cooling in the scattering, and the lower ones refer to heating. Since the curves of the kinematic relations differ in how they intersect the dispersion curve for different E_0, ε, and θ, to reduce the results on the peak widths and intensities to the condition $q=$const it is convenient to introduce the conversion coefficient j. When the dispersion curve and the kinematic relation are linear within the limits of the peak width, the conversion coefficient is

$$j=\cos\alpha\left[1-\left(\frac{dq}{d\varepsilon}\right)\mathrm{grad}_q\,\varepsilon(q)\right], \tag{1.3}$$

where $\varepsilon(q)$ is the dispersion curve, α is the angle of deviation of the kinematic curve from the vertical ε axis, and $dq/d\varepsilon$ is found from (1.2). The data on the widths W_q and intensities I_q of the peaks for $q=\text{const}$ are obtained by multiplying the results obtained for $\theta=\text{const}$ by j: $W_q=W_\theta j$, $I_q=I_\theta j$.

This transformation is possible in practice only for relatively narrow peaks; other approaches are required for wider ones. We note that the Waller–Froman expression[17] used earlier to transform data to the scale $q=\text{const}$ differs from (1.3) by the factor $\cos\alpha$, which is unimportant at high energies E_0 because $\alpha\sim 0$.

1.3. The cadmium technique

The background is usually measured by the *cadmium technique*.[18] A cadmium shutter placed in front of the mechanical chopper makes it possible to completely shut off the thermal neutron beam. Technically, the use of the cadmium technique amounts to the following: the measurements for both liquid ^{4}He and the empty cryostat are performed by alternating the two modes in which the cadmium shutter is open or closed. We shall discuss other important technical features of the measurements and spectrometer characteristics when we describe specific experiments.

It should be noted that the IBR-2 reactor offers the nontrivial possibility of studying liquid ^{4}He by neutron inelastic scattering in the region of energy transfers $\varepsilon\approx(1-1000)$ μeV and wave-vector transfers $q\approx(10^{-2}-1)$ Å^{-1} with an energy resolution $\Delta E<10$ μeV.[19] It is thought that this setup will operate for "very cold neutrons" ($E_0\leqslant 1$ meV), using the reverse-geometry method with multilayer monochromators as filters. Preliminary tests of the main components of the setup have indicated that this will work.

2. STRUCTURE OF THE EXCITATION SPECTRUM OF LIQUID ^{4}He

Landau was the first to suggest possible shapes of the excitation spectrum of a Bose liquid.[2] On the basis of the experimental fact that the specific heat of He II at temperature $T\to 0$ falls off as T^3, he postulated that near the ground state liquid ^{4}He can be treated as a set of individual elementary excitations or quasiparticles. At small wave vectors corresponding to sound quanta (phonons), the energy of the excitations depends linearly on the wave vector q, with the coefficient of proportionality equal to the speed of sound c:

$$\varepsilon(q)=c\hbar q. \tag{2.1}$$

The static structure factor $S(q)$ for liquid ^{4}He at small q and $T\to 0$ was obtained by Bijl,[20] Feynman,[21] and Pitaevskiĭ:[22]

$$S(q)=\hbar q/2Mc, \tag{2.2}$$

assuming that only one-phonon processes contribute to $S(q)$. For $T\neq 0$, $S(0)=\rho k_B T K_T$, where ρ is the density of ^{4}He atoms, k_B is the Boltzmann constant, and K_T is the isothermal compressibility.

At small oscillation frequencies ω, sound waves propagate under the conditions of local thermodynamical equilibrium, owing to frequent collisions between quasiparticles. In the limit $\omega\ll\nu$, where ν is the collision frequency, we have the hydrodynamical or *collision* regime, and a well defined first-sound mode can propagate. For $\omega\gg\nu$ collisions are rare (the *collisionless* regime), and density fluctuations are the high-frequency analog of ordinary sound, called *zero sound* by Landau. The damping of zero sound due to quasiparticle collisions is small, so that zero sound is a well defined mode propagating in a nonequilibrium medium. In the transition region between first and zero sound ($\omega\sim\nu$) collisions occur frequently enough to suppress the zero-sound mode, but not frequently enough that an undamped first-sound wave can propagate. Therefore, this transition region should correspond to the maximum of sound-wave absorption.

In the collisionless regime the curve corresponding to the excitation spectrum first goes upward, because the spectrum is described by the expression

$$\varepsilon(q)=c\hbar q+\gamma q^3+\ldots,\quad \gamma>0. \tag{2.3}$$

Then the group velocity of the excitations again decreases, and at some $q=q^*$ the spectrum intersects the first-sound line and goes under it. This shape of the spectrum at temperature $T\to 0$, i.e., in the absence of quasiparticle collisions, leads to a unique behavior of the damping of the excitations, which has been studied by Iordanskiĭ and Pitaevskiĭ.[23] As the spectrum deviates from the linear dependence, decay into two, three, and more excitations up to infinity becomes possible. As q increases it first becomes impossible to decay into two excitations, then into three, and then successively into larger numbers of excitations. There is therefore a sequence of thresholds which accumulate as the point q^* is approached. For $q\to q^*$ there can be decay only into an infinite number of phonons $n\to\infty$. For $q>q^*$ the excitation cannot decay into any number of phonons. Therefore, the point q^* is a "singular point" at which the decay or damping of the excitation vanishes. The probability for decay of an excitation near q^* is given by[23]

$$W_{\mathrm{IP}}\propto\left(\frac{\varepsilon^6\gamma}{\hbar^6\rho c^8}\right)^n\exp(-5n\cdot\ln n);\quad n=\frac{q^{3/2}\gamma^{1/2}}{(\varepsilon-c\hbar q)^{1/2}}. \tag{2.4}$$

Here the logarithm in the argument of the exponential decay law makes the damping even faster.

In the region $q\sim 1/a$, where a is the interatomic spacing, Landau predicted that the excitation spectrum of superfluid ^{4}He has a minimum:

$$\varepsilon(q)=\Delta+\hbar^2\cdot(q-q_r)^2/2\mu,$$

where μ is the roton effective mass. The damping of the excitations near the roton minimum as a function of temperature was studied by Landau and Khalatnikov,[24] who found that the width of the roton peaks is

$$W(T)=94\sqrt{T}\exp(-\Delta/k_BT), \tag{2.5}$$

where W is the full width at half-max.

The behavior of the excitation spectrum in superfluid ^{4}He at wave vectors beyond the roton region was studied by

Pitaevskiĭ.[25] As q increases the energy of the excitations reaches some threshold value (the end point of the spectrum), above which an excitation is unstable to decay into two or more excitations of lower energy.

Landau, Pitaevskiĭ, and Feynman obtained the excitation spectrum of superfluid ^{4}He without considering the Bose condensate. In the theoretical studies begun by Bogolyubov, the Bose condensate is introduced at the very beginning. According to the microscopic Bogolyubov theory, the presence of the Bose condensate leads to a dispersion curve $\varepsilon(q)$ of the phonon type at small wave vectors in the sense that the curve has a finite slope at the origin, i.e., $d\varepsilon/dq \neq 0$ for $q \to 0$. Here it should be remembered that the prediction that the spectrum is linear is obtained by assuming that there are no excitations of the ^{4}He atoms at zero temperature.

The microscopic theory of a Bose liquid has been developed by applying the technique of quantum field theory to a system of many Bose particles. Belyaev[5] determined the quasiparticle energy spectrum near the ground state for a system of interacting Bose particles at low density. At small q the quasiparticles are phonons, and in going to high excitations or large momenta a wave-like kink develops on the dispersion curve (for a gas of elastic spheres). This kink grows as the density of the Bose condensate increases, and at sufficiently high density first a bend develops, and then a maximum and minimum, so that the spectrum qualitatively resembles the Landau spectrum.

The theory of liquid ^{4}He was later developed by Hogenholtz and Pines,[26] Gavoret and Nozières,[27] Hohenberg and Martin,[28] Szepfaluzy and Kondor,[29] Griffin and Cheung,[30] and others. Two types of excitation were considered in these studies: density excitations of the particle–hole type (two particles) described by a dynamical susceptibility function χ, and quasiparticle excitations (one particle) described by a single-particle Green function G. Both quasiparticle excitations and particle–hole excitations are density fluctuations. For example, for strongly interacting liquids Gavoret and Nozières showed that both types of excitation χ and G at small q and $T=0$ have a common dispersion curve of the form $\varepsilon(q)=c\hbar q$. Szepfaluzy and Kondor and also Griffin and Cheung showed that for $T>0$ hybridization (mixing) of these excitations via the Bose condensate occurs.

Griffin, Glyde, and Stirling[31–36] proposed a somewhat different interpretation of the phonon–roton excitations observed in neutron experiments. In superfluid ^{4}He the general dynamical susceptibility χ has two components: a one-particle Green function G with weight in χ depending on the density of the Bose condensate $n_0(T)$, and the dynamical susceptibility χ' of the atoms above the condensate. The authors suggest that χ and G are also mixed via the Bose condensate. At small q the liquid is characterized by a collective mode of the zero-sound type, which was proposed by Pines[37] for liquids with strong interaction between the atoms. This mode exists in the normal and the superfluid phases of ^{4}He. As q increases the zero-sound mode widens, and it is very wide in the roton region in the normal phase. The quasiparticle excitations in the superfluid phase are well defined. They are manifested as a *sharp* peak at all q and vanish in the normal phase, where the amount of Bose condensate is $n_0(T)=0$.

Woods and Svensson[11] found that their results for the dynamical structure factor $S(q,\varepsilon)$ in superfluid ^{4}He in the maxon–roton region are described well by the expression

$$S(q,\varepsilon)=n_s S_s(q,\varepsilon)+n_n S_n(q,\varepsilon)\,\frac{1-\exp(-\varepsilon/k_B T_1)}{1-\exp(-\varepsilon/k_B T)};$$

$$n_s=\rho_s/\rho; \quad n_n=1-n_s, \tag{2.6}$$

where ρ_s is the density of the superfluid component. Here $S_n(q,\varepsilon)$ is the intensity of the peak of normal He I at $T_1>T_\lambda$. The thermal population factor is close to unity and is important only for $\varepsilon<k_B T$. The authors considered this assumption natural because the quantity $S(q,\varepsilon)-\rho_n S_n(q,\varepsilon)$ that they obtained experimentally at wave vectors $q=(1.5-2)$ Å^{-1} behaved as $A\rho_s$ ($A=$const) as a function of temperature. Equation (2.6) essentially implies that neutrons perceive the normal and superfluid components differently. Naturally, attempts were made to find a theoretical justification of this scattering picture.[38,39] However, so far no such justification has been found. Moreover, it is these studies which have served as the foundation for the Griffin–Glyde picture discussed above. On the other hand, the so-called Woods–Svensson decomposition (2.6) has had many ups and downs in subsequent experimental studies.[40,41] It turned out that the more correct inclusion of multiphonon contributions to the single-particle neutron scattering intensity leads to violation of the empirical decomposition rule. This appeared especially clearly in analyzing experiments performed at high pressure. This fact led to doubts about the Woods–Svensson idea of the decomposition of the scattering intensity into two components.

The results of our studies[42–45] indicate that the picture of a *sharp* neutron scattering peak in the form of a superposition of two components is correct in the superfluid phase in the phonon and maxon–roton regions of the spectrum when the contribution of the multiphonon part of the scattering is excluded. Here the peaks of the components have similar locations but different widths, so that to separate them it is necessary to have a very accurate mathematical description of the experimental peaks.

2.1. The technical possibilities of an experiment

We have attempted to use the new technical possibilities of the DIN-2PI spectrometer in conjunction with the special properties of ^{4}He itself. Let us describe the methodological features of the experiments that we have performed to study the excitation spectrum of liquid ^{4}He.

The resolution. An important parameter of the spectrometer is the width of the energy resolution function. For the time-of-flight technique this quantity depends on the energy of the neutrons incident on the sample E_0 and the energy of the scattered neutrons E:

$$\Delta E \propto \sqrt{aE_0^3+bE^3+\ldots}, \tag{2.7}$$

where a and b are constants. According to (2.7), better energy resolution can be obtained by making the energy of the incident neutrons as low as possible. The results of measure-

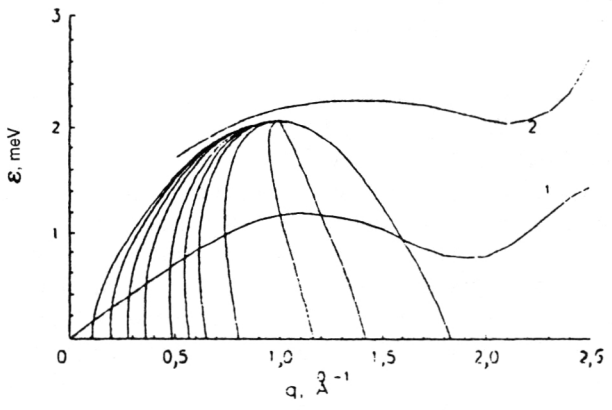

FIG. 3. Dispersion curve of single-particle excitations (1) and curve of the maximum of the peak in neutron multiphonon scattering (2). Kinematic laws for neutrons scattered at various angles for $E_0=2.08$ meV.

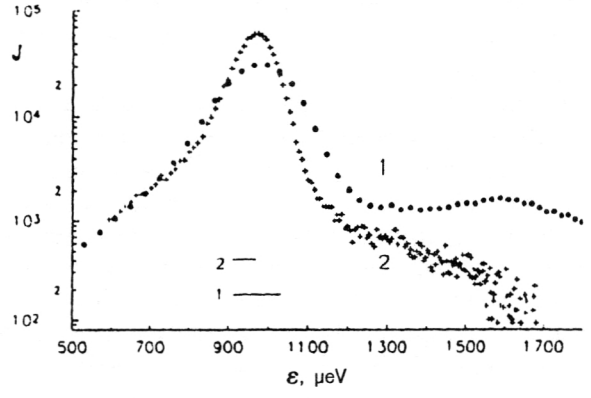

FIG. 4. Experimental spectra of neutron scattering by ^{4}He at $q=1.57$ Å^{-1}: (1) $T=1.5$ K and $E_0=3.5$ meV; (2) $T=1.45$ K and $E_0=2.08$ meV. The horizontal lines show the resolutions for each peak. The curves are normalized to the area of the single-particle peaks.

ments at the lowest temperature $T=0.42$ K and initial neutron energy approximately equal to 2 meV showed that the full width at half-max (ΔE) of the resolution function in the maxon region is less than 50 μeV, while in the roton–phonon region it is less than 100 μeV. Monte Carlo estimates of the width of the resolution function made by our colleagues at the Physics and Power Institute in Obninsk gave widths close to the experimental values at $T=0.42$ K.

Multiphonon scattering. When performing experiments it is necessary to remember that at energies above the dispersion curve of one-phonon excitations a broad band associated with the excitation of two or more quasiparticles begins. These are the so-called multiphonon or multiparticle processes. The q dependence of the maximum of this part of the scattering is given by curve 2 in Fig. 3. This scattering has a quite complicated structure and is interesting in itself.[46,47] The important thing for us is that the low-energy regions of multiparticle processes can affect the magnitude and form of the scattering conventionally referred to as one-phonon or one-particle scattering. This can be manifested especially clearly in the maxon region. As can be seen from Fig. 3, the initial energy of 2 meV lies below the band of multiparticle excitations in ^{4}He, so that processes creating them are significantly suppressed, and their low-energy parts make a small contribution to the single-particle neutron scattering intensity. This is illustrated clearly in Fig. 4, where for comparison we give the experimental spectra for $T\sim1.5$ K and $q\sim1.6$ Å^{-1} at two initial neutron energies: curve 1 is for $E_0=3.5$ meV, and curve 2 is for $E_0=2.08$ meV. The curves are normalized to the area of the single-particle peak.

We see clearly from Fig. 4 that as the initial neutron energy is lowered the width of the single-particle peak is significantly decreased and the contribution of multiphonon scattering is greatly diminished. It is probably not possible to get rid of multiphonon scattering completely, because the low-energy tail of multiphonon scattering lies under the single-particle excitation peak. Of course, further lowering of the incident neutron energy would decrease the contribution of multiphonon scattering even more. However, first, the intensity of the incident and, accordingly, of the scattered neutrons would decrease rapidly and, second and most important, the energy E_0 would approach or, more precisely, become comparable to the Debye temperature of liquid ^{4}He ($T_D\approx15$ K), which can lead to distortion of the shape of the single-particle peaks on the high-frequency side.

Here we must again return to the Woods–Svensson experiments.[11] For clarity, let us consider Fig. 5, taken from Ref. 41. Woods and Svensson relate the narrow peak to the superfluid component. They obtain the normal component from the wide peak, subtracting from it the part of the scattering which remains when the ^{4}He temperature is decreased to $T\sim1.2$ K. It is assumed that the part of the wide peak which depends on temperature pertains to scattering on the normal component. The part which remains after the temperature is lowered to $T\sim1.2$ K then pertains to multiphonon scattering, and as T is decreased further below 1.2 K this scattering changes only insignificantly. Our experiments show that, instead, all of the wide peak pertains to multiphonon scattering. There is no contradiction in this. The wide peak attributed to scattering on the normal component

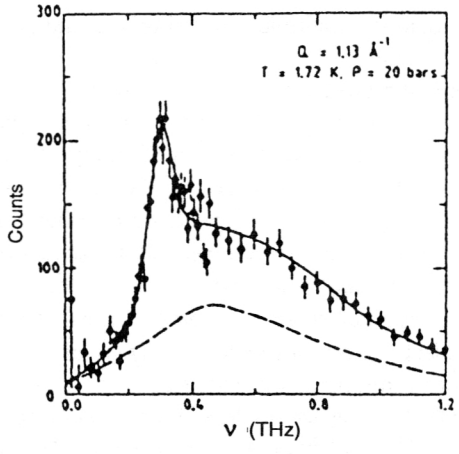

FIG. 5. Comparison of the spectra of neutrons scattered on superfluid ^{4}He (points) with the description by the Woods–Svensson model (solid line). The dashed line shows the normal component $n_nS_n(q,\omega,T)$ (Ref. 41).

also pertains to multiphonon scattering with the only difference that neutrons are scattered on excitations already present in the liquid.

Multiple scattering. We have worked with a sample of liquid ^{4}He which is rather large ($V\sim3600$ cm^3) compared with those of other authors ($V\sim60$ cm^3). On the one hand, this gives a gain of about 60 in the intensity, but, on the other, this can in principle make neutron multiple-scattering processes more important and distort the true shape of the peak. To see how important these effects are, *first* we performed special experiments with a cadmium insert in the sample container dividing the volume into a series of thin layers (2 cm wide). Comparison of the results of measurements with and without this insert did not reveal any noticeable differences in the shape of the scattering peaks. The scattering intensity was decreased by about 7%, owing to cutoff of the neutron beam due to the thickness of the cadmium layers. *Second*, lowering of the incident neutron energy decreases the total cross section for neutron scattering.[48] For example, for $E_0=2.08$ meV, the cross section is $\sigma_{\text{tot}}\approx0.2$ b and the sample transmission is 0.94. The neutron energy E_0 was selected so that the probability of repeated scattering in ^{4}He continued to fall, owing to decrease of the total cross section with decreasing energy. Moreover, if after the first scattering the neutron energy becomes somewhat smaller than the energy of the excitations in the maxon, then subsequent scattering becomes possible only in a restricted solid angle. In addition to these factors which reduce multiple scattering, there is another. In the study of inelastic processes, multiple scattering becomes important if neutrons can undergo elastic scattering in the sample, i.e., scattering without a change of energy. In this case, owing to the relatively large cross section for elastic scattering, it is necessary to take into account such possibilities as elastic plus inelastic or inelastic plus elastic scattering. In this sense superfluid ^{4}He is exceptional when compared with other liquids: up to now, elastic scattering has not been observed experimentally. Therefore, in superfluid ^{4}He multiple scattering can be associated only with inelastic processes. If for the first scattering $n\sigma_{\text{tot}}x\approx0.06$, then the subsequent scattering is less than 3% of the first $[n\sigma_{\text{tot}}(x/2)\leqslant0.03]$, and it can be assumed that effects of neutron multiple scattering are unimportant in these experiments.

Let us make the following remark. In condensed media the total cross section for neutron scattering at energies of the order of several meV falls off very abruptly. This drop is usually associated with a decrease of the neutron elastic coherent scattering at wavelengths $\lambda>2d$, where d is the maximum distance between planes. Elastic scattering is not observed in superfluid ^{4}He, and the abrupt decrease of the total cross section at energies of order 2 meV is mainly related to inelastic processes or to a decrease of the contribution of neutron multiphonon scattering.

We note that the use of low incident neutron energies leads to an additional improvement of the *background conditions* of the experiment, owing to the large neutron time of flight, because the measurements are made longer after the power pulse of the reactor. A rotating chopper placed near the active zone of the reactor plays a fundamental role in suppressing the background.

The uncertainty in the value of q associated with the finite sample and detector sizes is $\Delta q\sim0.06$ Å^{-1} at small q, and smaller at large q. Some of the experiments were performed with $\Delta q\sim0.02$ Å^{-1}.

Therefore, by using low incident neutron energy we improved the resolution function and the background conditions. It was possible to suppress multiparticle processes in neutron scattering, to significantly improve the accuracy of the measurements, and to actually observe and analyze features of the neutron scattering spectra at a scale $(1-5)\times10^2$ times smaller than the intensity in the main single-particle scattering peak. The experimental possibilities are illustrated by the fact that in these experiments we observed and analyzed peaks associated with neutron scattering in liquid ^{4}He involving an energy gain, i.e., peaks corresponding to cases where the neutrons were heated in the liquid.

2.2. Experimental results

Description of the shape of the peaks in neutron inelastic scattering. The dynamical structure factor $S(q,\varepsilon)$ defined in (1.1) was calculated from the experimental data using the expression

$$S(q,\varepsilon)\propto(E_0^2/E^2)d^2J(\theta,t)/d\Omega dt.$$

It is convenient to analyze the scattering spectra for the *superfluid* and *normal* phases of liquid ^{4}He separately. In addition, we can distinguish *three* characteristic regions of the wave vector q for which the shapes of the peaks also differ. They are: the initial *phonon* segment of the dispersion curve $q<0.4$ Å^{-1}, the *maxon–roton* excitation region $q>0.65$ Å^{-1}, and, finally, the *transition* region $0.4<q<0.65$ Å^{-1}, which we shall refer to as region Y.

The peak shape was analyzed using either Gaussians (GG) or Lorentzians (LG). The notation GG and LG means that the intrinsic Gaussian or Lorentzian shape is convolved with the Gaussian describing the spectrometer resolution function. At present it is difficult to choose between these two models within the error when analyzing some peaks, although if a measured peak is rather clearly distinguished, the Lorentzian shape is preferable because it gives a better description of the edges of the peak.

Regarding the description of the peak shape using the "harmonic oscillator" (HO) function,[34] at energies of about $\varepsilon\geqslant0.4$ meV this description differs insignificantly from the LG description. As the temperature of liquid ^{4}He is decreased, the conditional energy ε at which these descriptions are about the same is lower. At low energies the difference between the LG and HO descriptions becomes more noticeable from the side of low excitation energies. The HO function, which simultaneously describes both the neutron cooling spectrum and the neutron heating spectrum (if, of course, the heating spectrum is observed), is convenient for describing the experimental data obtained for $q=$ const. In our case, where $\theta=$ const and $q\neq$ const, the description of the peak

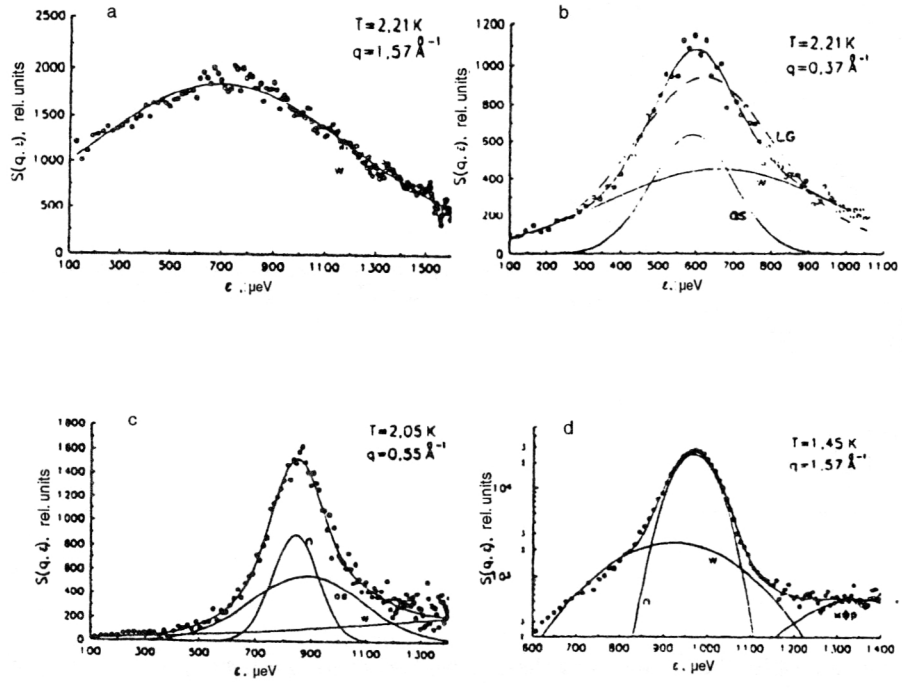

FIG. 6. Curves $S(q,\varepsilon)$ at various temperatures and their components for various q. For comparison, in (b) we show the description by a single LG.

shapes by the HO function is complicated by the fact that the curves of the kinematic relations for neutron cooling and heating do not coincide.

The superfluid phase. In the *maxon–roton* region of the spectrum the *sharp* single-particle neutron scattering peak is poorly described by a single Gaussian (GG) or a single Lorentzian (LG). The best description from the viewpoint of the statistical criteria of the approximation (the value of χ^2, the correlation coefficients of the model parameters, and so on) corresponds to a model of two Gaussians (GG+GG) or two Lorentzians (LG+LG). The two components of the scattering peak differ significantly in width, and so henceforth we shall refer to one of them as narrow (n) and to the other as wide (w). Typical examples of the decomposition are shown in Fig. 6.

A narrow and a wide component of the neutron scattering are also observed in the *phonon* region of the spectrum. For reasons which will become clear later, here the narrow component apparently has an origin different from that of the n component, and we shall denote it by os. The wide component (w) is clearly visible in this region only near T_λ, and at lower temperatures its intensity falls and it becomes difficult to distinguish.

In the *transition* region Y the picture of neutron scattering is more complicated. Interpolating the description of the peaks by the n, os, and w components in the transition region Y, we find that apparently the three scattering components n, os, and w are directly observed here. The os component begins to be strongly damped with increasing q, and near the upper limit of the region for $q\sim0.65$ Å^{-1} it becomes difficult to distinguish. As q decreases and the lower limit of the region is approached, the parameters of the n component approach those of the os component, and for $q<0.4$ Å^{-1} these components become difficult to separate. The wide component (w) is present in this region but is less clearly manifested than in the phonon or maxon–roton regions, and it is probably also damped out.

The normal phase. Only wide scattering peaks (w) described well by a single GG or a single LG are observed above T_λ in the *maxon–roton* region. In addition to the wide component (w), the narrow os component is clearly seen in the *phonon* region. In the *transition* region Y the os component begins to be damped out rapidly, and above $q\sim0.65$ Å^{-1} it is no longer observed. The wide component (w) is poorly visible in the transition region. The narrow component (n) characteristic of He II is not seen at all above T_λ.

Errors. The statistical errors are shown in the figures. The peak locations are determined with high accuracy, and the errors are smaller than the points on the graphs. They are somewhat more difficult to determine at very small $q\sim0.1$ Å^{-1} when performing experiments with $\Delta q=0.06$ Å^{-1}. The parameters of the wide peaks (w) in the region Y are determined less accurately, especially at high temperatures, because the widths of these peaks become comparable to the incident neutron energy. The main systematic error is associated with the inclusion of the contribution of multiphonon scattering, in spite of its small magnitude. This mainly affects the maxon region, because this region is closest to the maximum of the multiphonon peak. It also affects the determination of the parameters of the w component at low temperatures, owing to the low intensity of this component. Systematic error can also arise from the model used to analyze the experimental results.

The dispersion curves. Let us first consider the *maxon–roton* region of the spectrum for $q>0.65$ Å^{-1}. In the *superfluid* phase the dispersion curves of the narrow (n) and wide (w) components are close to each other. The difference between $\varepsilon_n(q)$ and $\varepsilon_w(q)$ is less than 10%. However, a tendency for the entire dependence $\varepsilon_w(q)$ to shift to smaller q relative to $\varepsilon_n(q)$ is observed at all temperatures $T<T_\lambda$. Be-

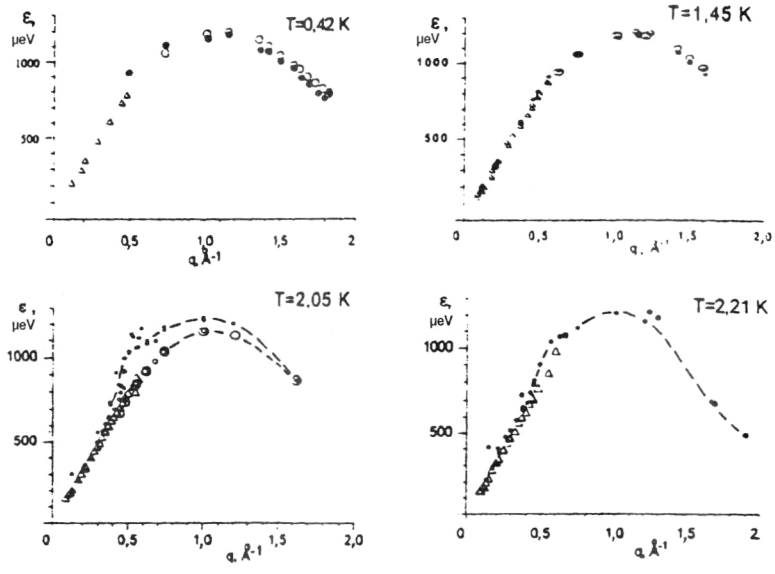

FIG. 7. Dispersion curves at various T for the n (light circles and squares), w (dark circles), and os (triangles) components.

cause of this, the maxima in the maxon and, probably, the roton minima of the n and w dispersion curves do not coincide (see Fig. 7). The temperature dependences are rather weak for these two components. However, we note that whereas at low temperatures in the maxon the n component lies above the w component, near the λ point they change places. In passing through T_λ the n component vanishes, while the dispersion curve $\varepsilon_w(q)$ does not change significantly (see Fig. 8b).

In the *phonon and transition* (Y) regions of the spectrum the dispersion laws for the n and os components are the same (Fig. 7). The dispersion curve for the wide component $\varepsilon_w(q)$ lies above $\varepsilon_{os}(q)$. The temperature dependences of $\varepsilon_{os}(q)$ and $\varepsilon_w(q)$ in this part of the spectrum are also very weak and practically do not feel the transition to the normal phase (see Fig. 8a).

The integrated intensities. In the *superfluid* phase the dependences of the integrated intensities on wave vector for the narrow and wide components $Z_n(q)$ and $Z_w(q)$ in the *maxon–roton* region are similar. As an illustration, in Fig. 9 we show these dependences for $T=0.42$, 1.45, and 2.05 K. The two curves obviously have the well known maximum[7,49] in the vicinity of the roton minimum of the dispersion curve, which is shown in Fig. 10 for the one-component description of the sharp peak.

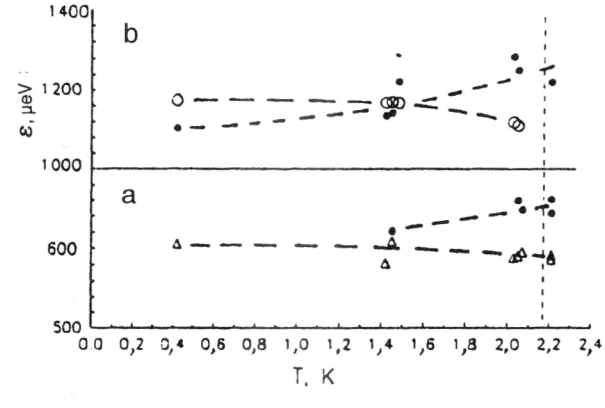

FIG. 8. Change of excitation energy with temperature: (a) $q=0.37$ Å^{-1}; (b) $q\sim1$ Å^{-1} for the n (light circles), w (dark circles), and os (triangles) components.

Analysis shows that at any temperature the ratio of the intensities $\eta(q)=Z_n(q)/[Z_n(q)+Z_w(q)]$ is independent of q within the point spread (Fig. 11). However, this ratio depends strongly on temperature (see Fig. 12).

In Fig. 13 the dependences $Z_n(T)$ and $Z_w(T)$ are shown for $q\sim1.6$ Å^{-1}. We see from this figure that the narrow component of the scattering dominates at low temperatures, and actually vanishes as T_λ is approached. Conversely, the intensity of the wide component falls off sharply with decreasing T.

Only wide scattering peaks (w) remain in the *normal* phase of liquid ^{4}He, and for them the dependence $Z_w(q)$ (Fig. 14) is similar to that for the wide component in the superfluid phase.

Now let us turn to the *phonon part* of the dispersion curve for $q<0.65$ Å^{-1}. The temperature dependences $Z_{os}(T)$ for different values of q (see Fig. 15) differ from the analogous dependences $Z_n(T)$ (see Fig. 13) in that for $T>T_\lambda$ the values of $Z_{os}(T)$ do not vanish. On the basis of this we can assume that in the superfluid phase the narrow component (os) in the phonon part itself consists of two components with similar locations and widths: a narrow scattering peak (os) whose intensity probably depends weakly on temperature, and a narrow peak (n) whose intensity varies with temperature in the phonon region as in the maxon–roton region.

We noted earlier that Bijl[20] and Feynman[21] established a relation between the structure factor of liquid ^{4}He and the collective excitation spectrum (2.2). The same result was obtained by Pitaevskiĭ on the basis of the hydrodynamics of a quantum liquid.[22] To check that this relation is satisfied, we did the following. By summing all the components we obtained data on the integrated intensities at temperatures

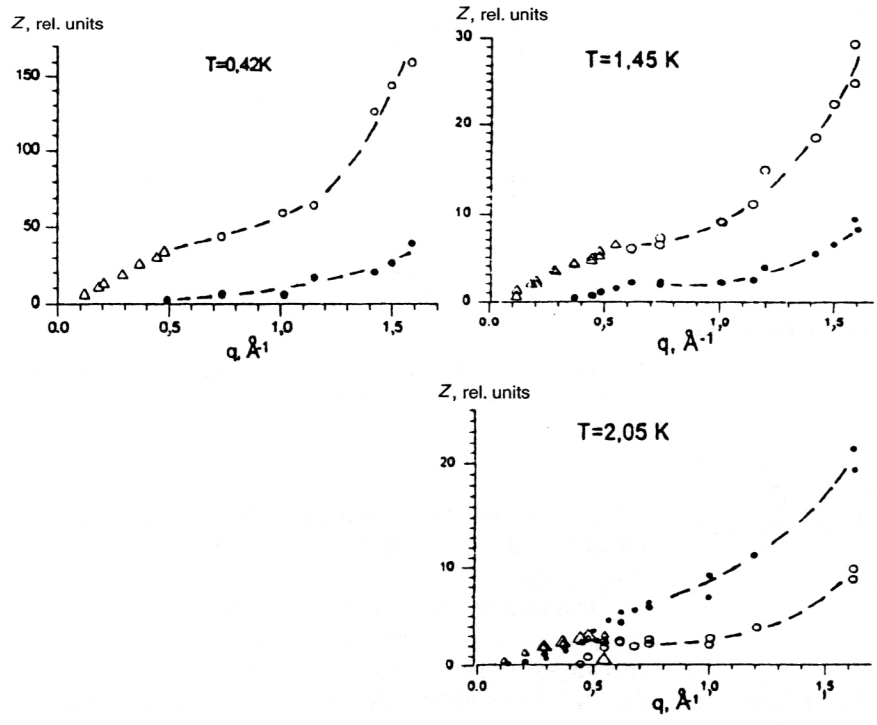

FIG. 9. Dependence of the intensity on q at $T=0.42$, 1.45, and 2.05 K for the n (light circles), w (dark circles), and os (triangles) components.

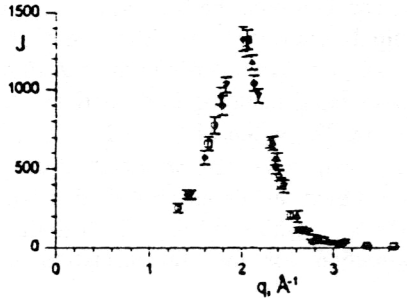

FIG. 10. Dependence of the intensity on q at $T=1.2$ K in the region of the roton minimum, taken from Ref. 49.

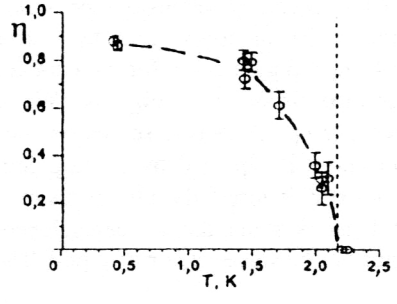

FIG. 12. The dependence $\eta(T)$.

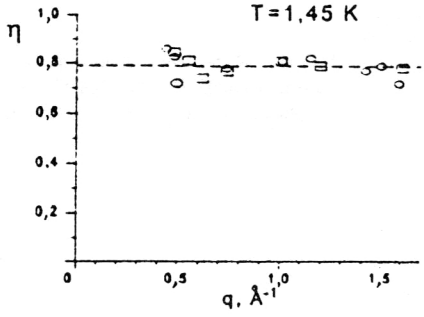

FIG. 11. The curve $\eta(q)$ at $T=1.45$ K. The dashed line is the average value.

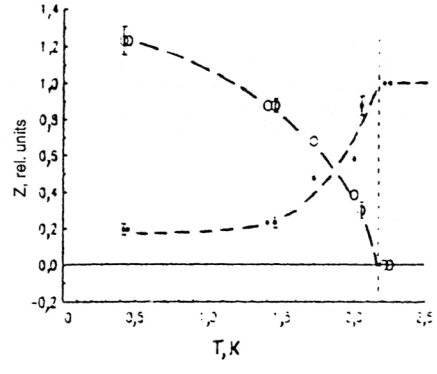

FIG. 13. Temperature dependence of the intensity for the n (light circles) and w (dark circles) components. The curves are normalized to unity for the w component at $T>T_\lambda$.

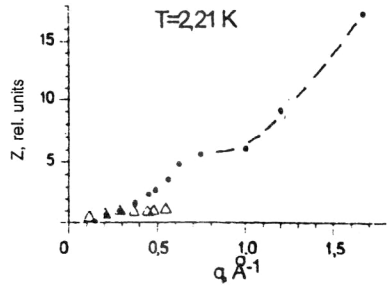

FIG. 14. Dependence of the intensity on q at $T=2.21$ K for the w (dark circles) and os (triangles) components.

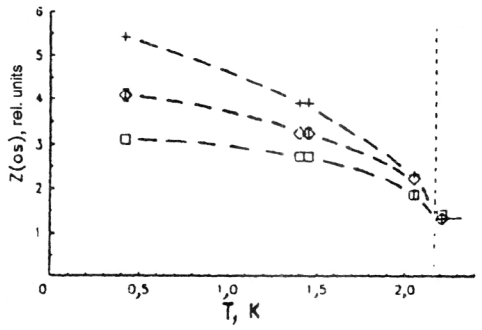

FIG. 15. Variation of the intensity of the os component with temperature: $q=0.28$ Å^{-1} (squares), $q=0.37$ Å^{-1} (diamonds), and $q=0.45$ Å^{-1} (plus signs).

$T=0.42$, 1.45, 2.05, and 2.21 K taking into account both cooling and heating of the neutrons in scattering. The phonon part of these data for $q\approx(0.1-0.6)$ Å^{-1} was described by two functions:

$$Z_1(q)=a_1+a_2q,$$

$$Z_2(q)=b_1+b_2q+b_3q^2,$$

where a_i and b_i are constants. The statistical criteria for the quality of the approximation χ_i^2 were obtained for both curves. Then we constructed the temperature dependence of the so-called dispersion relation[99] $v^2=\chi_1^2/\chi_2^2$, which characterizes the degree to which the experimental data deviate from a straight line. In Figs. 16a and 16b we show the dependences of the integrated intensities on wave vector and the description of the phonon regions by a straight line for the data at 0.42 K and by a curve for the data at 2.21 K. The T dependence of v^2 is shown in Fig. 16c. We see from this figure that as the temperature is raised below the λ point, the fairly smooth curve is replaced by a sharp jump near T_λ. The point at $T=0$ K is inserted on the basis of the theory of Refs. 20–22. It can be stated that the dependence of the static structure factor on the wave vector of liquid ^{4}He in the phonon region tends to a straight line as the temperature is decreased, and at the phase-transition point it undergoes a sharp jump.

The widths. The widths of the peaks for the n, os, and w components obtained by decomposing the scattered neutron spectra are shown in Fig. 17 for $T=0.42$, 1.45, 2.05, and 2.21 K. The width W is defined as the full width at half-max. The intrinsic values of the peak widths $W_{in}(q,T)$ were obtained by subtracting the peak widths at the lowest temperature $T=0.42$ K from the experimental widths $W(q,T)$. The $W(q,T)$ were obtained from measurements at $\theta=$const. The width of the n component has a minimum in the vicinity of the maxon associated with the best energy resolution due to the lowest final neutron energy. The width of the narrow component (os) increases sharply in the *transition* region Y, which indicates rapid damping in a relatively narrow range of wave vectors. The width of the wide component (w) depends strongly on q in the *phonon* region of the spectrum. In the *transition* region, as already noted, this component apparently has a large width and is difficult to distinguish.

The correction for the transformation to the scale

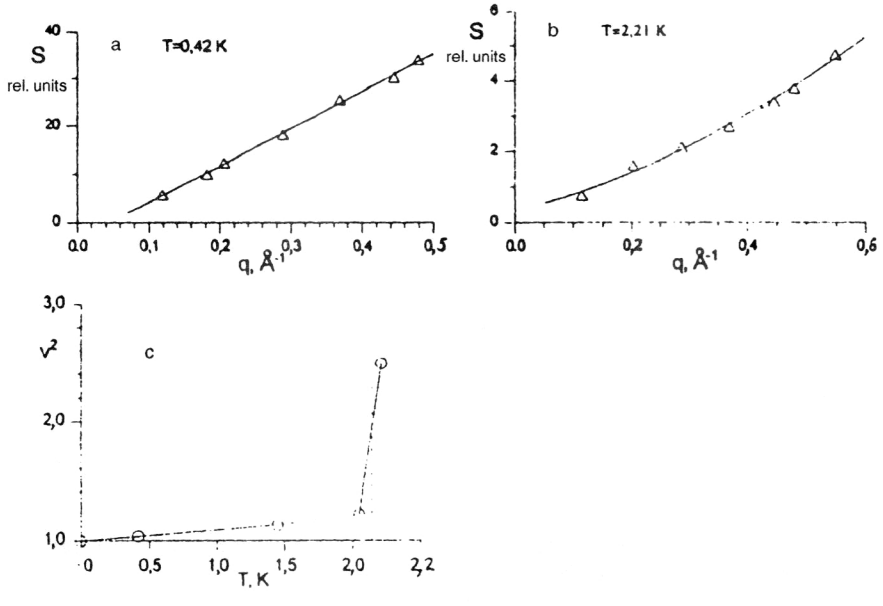

FIG. 16. Dependence of the integrated intensities on q at $T=0.42$ and 2.21 K and curves describing the phonon region; v^2 as a function of T.

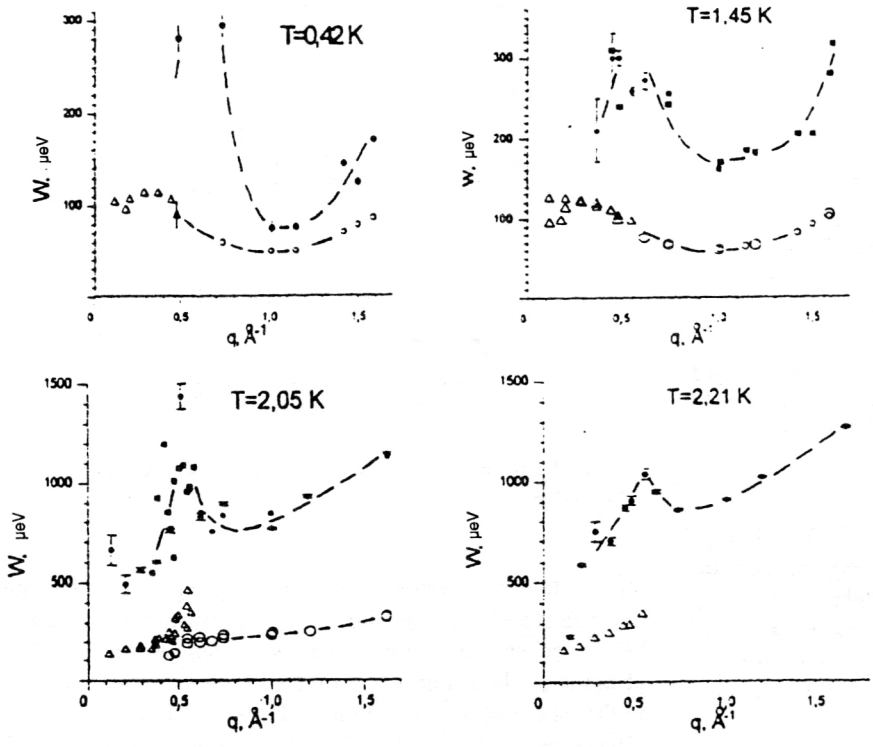

FIG. 17. Dependence of the peak widths on q for $T=0.42$, 1.45, 2.05, and 2.21 K for the n (light circles), w (dark circles), and os (triangles) components. The squares are the w component measured for $\Delta q \sim 0.02$ Å^{-1}.

$q=$const was not introduced, owing to the large values of $W(q,T)$, i.e., to the high degree of nonlinearity of the kinematic relation within the limits of the peak width, which could lead to distortions. We also did not include the correction associated with the uncertainty Δq. We recall that, owing to the different nature of the intersection of the kinematic relation and the dispersion curve at different neutron scattering angles, we obtain a deformed picture of the dependence $W(q)$. If it were possible to correctly introduce a correction to eliminate this deformation, i.e., to go to the scale $q=$const, then in the *maxon–roton* region of the spectrum we would probably have functions $W_n(q)$ and $W_w(q)$ weakly dependent on q at all temperatures. All the components of neutron scattering in ^{4}He have fairly strong temperature dependence of the width (see Figs. 18a and 18b).

The neutron heating spectrum. The study of liquid ^{4}He by means of neutron inelastic scattering has now become possible not only when neutrons are cooled in the liquid, but also when they are heated. When neutrons are heated, information is obtained on the excitations present in the liquid, while the cooling of neutrons itself creates such excitations. Here we shall discuss the results pertaining only to the low-energy part of the phonon curve. This is because the intensity of the scattered neutrons is proportional to the level population, and owing to the low temperature of the liquid such measurements can be carried out only at very small excitation energies. Measurements of the inelastic scattering spectra in neutron heating and cooling allow the use of the *principle of detailed balance* to study these processes. Here, of course, it should be remembered that since the measurements are made at $\theta=$const, the kinematic relations for neutron cooling and heating in principle do not coincide.

Experiments on neutron inelastic scattering with heating and cooling were performed at low incident neutron energies $E_0=1.83$ and 2.08 meV. The intensity of multiphonon and multiple processes is negligible, and the low level of background made it possible to perform measurements at wave

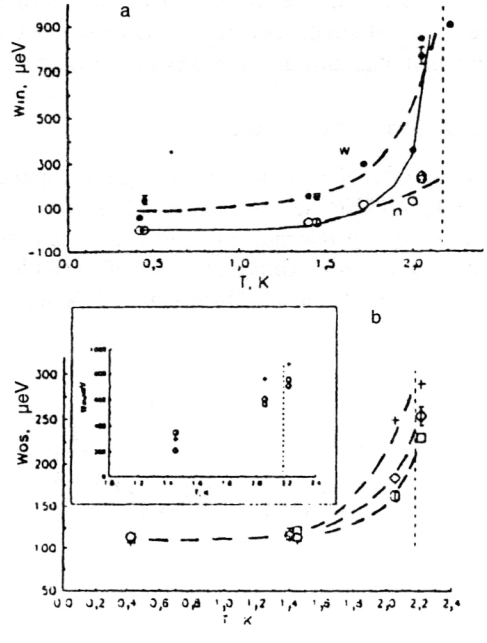

FIG. 18. Temperature dependence of the peak widths: (a) $q\sim 1$ Å^{-1} for the n (light circles) and w (dark circles) components. The resolution has been subtracted. The solid line was calculated for the roton widths using Eq. (2.5). (b) The os component and the w component (insert): $q=0.28$ Å^{-1} (squares), $q=0.37$ Å^{-1} (diamonds), $q=0.45$ Å^{-1} (plus signs). The resolution has not been subtracted.

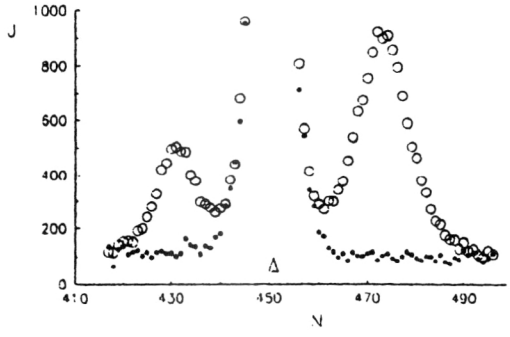

FIG. 19. Experimental spectrum of neutron inelastic scattering by liquid ^{4}He at $T=2.05$ K, $\theta=7.6°$, and $E_0=1.83$ meV (light circles) and the background without ^{4}He (dark circles). The arrow indicates the center of the elastic peak. N is the number of the time channel.

vectors $q>0.08$ Å^{-1} with uncertainty $\Delta q\sim 0.02$ Å^{-1}. In Fig. 19 we show the experimental spectrum of neutron inelastic scattering on liquid ^{4}He at the scattering angle $\theta=7.6°$ and sample temperature $T=2.05$ K, and also the background without ^{4}He. The right-hand peak pertains to neutron cooling, and the left-hand one to heating. The central peak comes from the background.

The dynamical structure factor for neutron heating $S(q,-\varepsilon)$ is related to that for cooling $S(q,\varepsilon)$ by the population factor:

$$S(q,-\varepsilon)=S(q,\varepsilon)\exp(-\varepsilon/k_BT). \tag{2.8}$$

Knowledge of $S(q,-\varepsilon)$ and $S(q,\varepsilon)$ allows use of (2.8) to calculate the temperature, which can then be compared with that measured experimentally by a thermocouple. We see from Fig. 20 that the calculated temperature coincided with the temperature $T=2.05$ K measured by the thermocouple. The larger error at small and large ε is associated with the relatively small statistics at the edges of the peak.

2.3. Discussion of the results

In summarizing the analysis of the experimental data, we note that in liquid ^{4}He there are apparently *two* characteristic regions of significant rearrangement of the energy spectra of the excitations and *three* different types of excitation, n, os, and w, which are manifested differently, depending on the

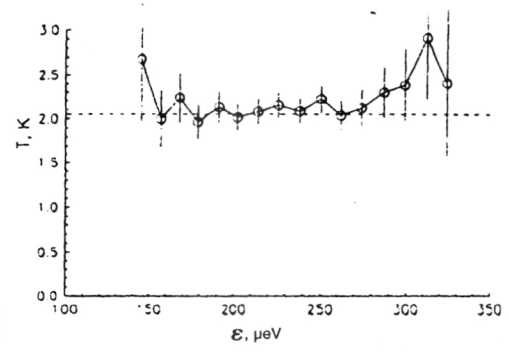

FIG. 20. Dependence of the calculated values of T on ε obtained from the experimental data on $S(q,\varepsilon)$. The sample temperature was $T=2.05$ K.

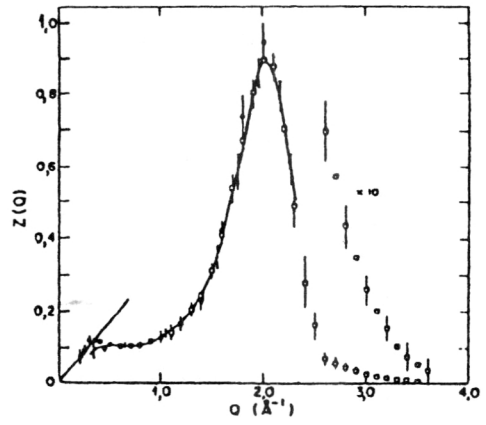

FIG. 21. Contribution of the intensity of one-phonon excitations[7] to $S(q)$ for $T=1.1$ K.

temperature and wave vector. First, strong qualitative and quantitative changes in the nature of neutron scattering in helium occur in a very narrow range of temperatures or right at the superfluid transition point T_λ. Second, clear changes in the nature of the excitations in both superfluid and normal ^{4}He occur in a narrow range of wave vectors (0.5–0.65) Å^{-1} in going from phonons to maxons.

The decomposition of the *sharp* neutron scattering peak into several components with completely different dependences $\varepsilon(T)$, $Z(T)$, and $W(T)$ proposed in Refs. 42–44 is a new result. Such a mathematical decomposition was necessary because the locations of these components in $\varepsilon-q$ coordinates turned out to be close to each other. Meanwhile, this decomposition became possible because the intensities and widths of these components have different temperature dependences and often differ significantly in magnitude. It would probably be possible to observe the two-component structure of the spectrum of neutrons scattered on liquid ^{4}He directly in experiment without the decomposition procedure if the maxon–roton peak were measured with a spin-echo spectrometer.[50]

There is some difficulty in directly comparing our experimental results with the data of other authors. In earlier studies the *sharp* peaks in neutron scattering in ^{4}He were, as a rule, described as one-component structures. It is useful to compare our results for $Z(q)$ with the data obtained by Cowley and Woods.[7] Direct comparison is rather difficult, owing to the difference in temperatures and wave vectors. The dependence $Z(q)$ at $T=1.1$ K from Ref. 7 is shown in Fig. 21. If we sum the intensities of all the components using our data at $T=1.45$ K, we obtain a very similar q dependence. The most precise measurements of other authors in recent years were made only for certain selected values of the wave vector. For example, at saturated-vapor pressure they are $q=0.4$ Å^{-1} (phonons) and $q=1.92$ Å^{-1} (rotons).[40] Our data on the parameters of $\varepsilon(q)$, for example, for $q=0.37$ Å^{-1} (see Fig. 7), are in good agreement with Ref. 40. In their experiments, Mezei and Stirling[51] obtained very accurate results for the intrinsic peak widths, which coincide very closely with the theoretical curve calculated by Landau and Khalatnikov[24] using (2.5) for the one-component description

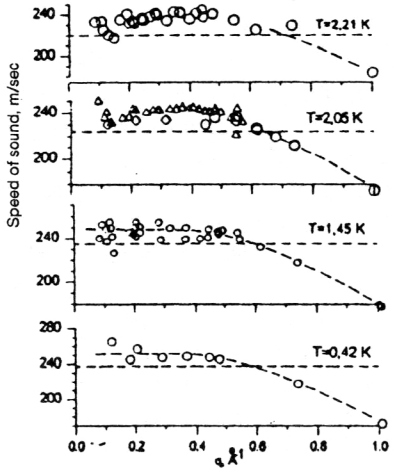

FIG. 22. Speed of sound at four temperatures for the os+n components. The horizontal lines indicate the speed of first sound.[52]

of the peak. Our results agree with the calculations for the widths of the n component at $T \leqslant 1.7$ K and are close to the widths of the w component for $T \geqslant 2$ K (see Fig. 18a).

Measurements at the passage through the λ point. For $T < T_\lambda$ a new component (n) is added to the complicated structure of the dispersion curves in He I. This component is not observed above the phase-transition point. The intensity of this branch for $q > 0.65$ Å^{-1} increases sharply with decreasing temperature and becomes dominant at low T. However, we note that even at the lowest temperature $T = 0.42$ K the intensity of the w component does not vanish, and $\eta \approx 0.88$ (see Figs. 12 and 13). In the phonon region the intensity of the w component is not observed at low temperatures within the errors.

The transition region Y. The neutron scattering components that we observed in the *transition region Y* of wave vectors (0.4–0.65) Å^{-1} have singularities. The os component is damped out rapidly. The wide component (w) has singularities in the dependences $\varepsilon_w(q)$, $W_w(q)$, and $Z_w(q)$ (see Figs. 10, 12, 17, and 21). The narrow component (n) seems to merge with or transform into the os component. The anomaly of the dispersion curve disappears in this region of q, i.e., the dispersion curve intersects the line of first-sound speed.

We have already mentioned the study of Iordanskiĭ and Pitaevskiĭ,[23] in which the behavior of the parameters of the dispersion curve for positive anomalous dispersion was studied. This problem was also actively discussed long ago in Ref. 53. In Refs. 54 and 55 it was found that precise measurements of $\varepsilon(q)$ in the phonon region indicate that this dependence on some segment lies above the line $\varepsilon = c\hbar q$. These measurements were performed at temperatures (1.1–2.3) K. The phenomenon where the phase velocity of the excitations exceeds the speed of first sound is referred to as anomalous dispersion. According to the data of our study, shown in Fig. 22 for different temperatures and the narrow component (os and n), anomalous dispersion is observed for $T \leqslant 1.45$ K for all the measured wave vectors $0.08 < q < 0.65$ Å^{-1}. For $T = 2.05$ and 2.21 K and $q < 0.3$

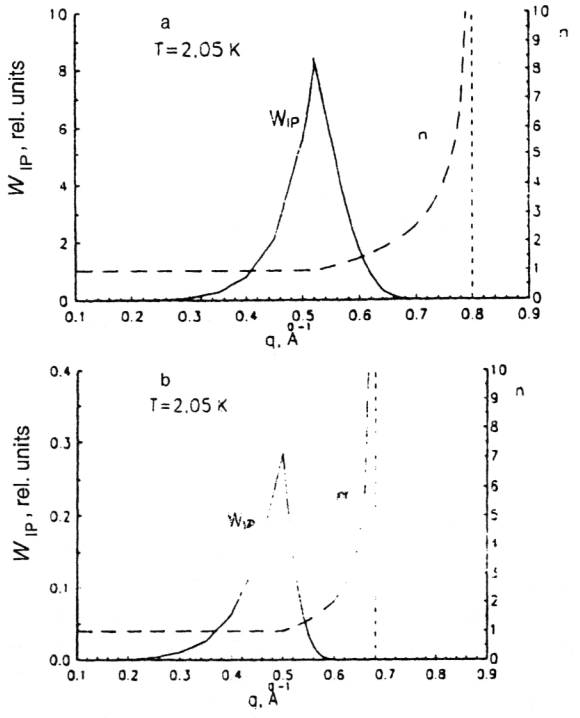

FIG. 23. Dependence of the calculated W_{IP} and n on wave vector for (a) the w component and (b) the os+n components. The figures have been normalized together. The vertical lines indicate the values of q^*.

Å^{-1} the dispersion curve approaches the line of first-sound speed, i.e., the region of the transition from zero to first sound is probably seen. Here it is also important to note that the dispersion curve intersects the line of first-sound speed in the region $q \sim (0.6–0.7)$ Å^{-1}. As the temperature decreases the intersection point moves to lower q. In general, these results are completely consistent with the data of the most accurate earlier measurements[55] if the sharp peak is assumed to have a one-component structure. The picture of the anomalous dispersion for the w component is the most interesting. The dispersion curve for the w component lies above the curves for the os and n components, and, in addition, an abrupt change of its slope in the Y region is observed.

The expressions obtained in Ref. 23 are universal: they can be used both for liquid ^{4}He and for other liquids. We shall use them for the n, os, and w components separately. As an example, let us consider the w component at $T = 2.05$ K. From the dispersion curve we find $q_w^* = 0.80 \pm 0.02$ Å^{-1}. We calculate the value $\gamma_w = (\varepsilon - c\hbar q)/q^3 = 2.26$ meV·Å^3, where c is the speed of first sound. Accordingly, for the os+n components we have $q_{os+n}^* = 0.68$ Å^{-1} and $\gamma_{os+n} = 0.50$ meV·Å^3. In Figs. 23a and 23b we show the dependences of the calculated values of $n(q)$ and $W_{IP}(q)$ from Eq. (2.4) for the w and os+n components. We see from this figure that the minimum number of photons n into which excitations decay for $q < 0.5$ Å^{-1} is nearly equal to unity, but then it increases sharply and becomes infinite as q^* is approached. The probabilities for decay of excitations into phonons $W_{IP}(q)$ have the form of peaks with a maximum at $q \approx 0.5$ Å^{-1}. In Fig. 17 we see a

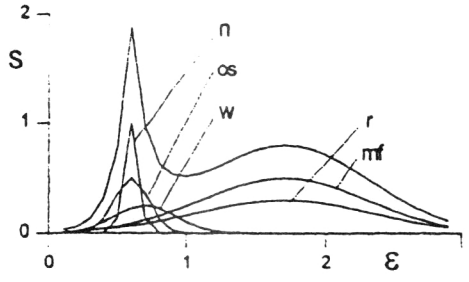

FIG. 24. Schematic spectrum of neutrons scattered on liquid ^{4}He and its components.

peak at $q \approx 0.5$ Å^{-1} for the w component, which can be taken as the peak for the decay of excitations into phonons. This peak is not observed experimentally for the os+n components, because its height at the maximum is about 30 times lower than that of the w component (see Fig. 23b). Other experimental conditions are probably necessary for observing it. In addition, we note that the peak width for the os +n components is considerably smaller than for the w component. Of course, the probability for decay into phonons is superimposed on the probability for the other process associated with interactions between excitations, and in Fig. 17 we see the sum.

Formation of the structure of the excitation spectrum of liquid ^{4}He. Analysis of the results of our studies,[42–45] the Woods–Svensson study,[11] and the Griffin–Glyde studies[31–35] shows that the spectrum of neutrons scattered by liquid ^{4}He consists of *sharp* and *wide* peaks, which in turn consist of n, os, and w components and r and mf components. In Fig. 24 we schematically show all these excitation peaks. Two excitation branches are seen in the normal phase of liquid ^{4}He in the vicinity of the sharp peak. One of them (w) is observed throughout the range of studied wave vectors q and is characterized by large peak width. The second branch (os) is seen clearly at small q and is rapidly damped out for $q \sim (0.5–0.6)$ Å^{-1}. These two branches are also characteristic of superfluid ^{4}He. Their dispersion laws and the behavior of the intensities and widths as functions of q are very similar to the corresponding dependences for the normal phase. In the superfluid phase an additional branch corresponding to the narrow component (n) appears along with the two neutron-scattering components discussed above. The r and mf components, which in these experiments are strongly suppressed, are also observed in both phases of liquid ^{4}He.

What is the physical interpretation of all these excitation branches? Let us discuss some ideas about this.

The *narrow component* (n), observed only in the superfluid phase of ^{4}He, can be uniquely associated with the canonical Landau dispersion curve for elementary excitations. As can be seen from Figs. 12 and 13, the intensity of this component depends strongly on temperature, and at low T it actually dominates the entire picture of neutron scattering in helium. The narrow component (n) is clearly visible in the maxon–roton region of the spectrum down to $q \sim 0.4$ Å^{-1}, where it approaches the os component, and at lower q it is observed together with the os component.

The *narrow component* (os) characteristic of the small-q region in both the normal and the superfluid phases of liquid ^{4}He is probably a branch of collective excitations of the zero-sound type. This question has been discussed in detail in a number of studies, for example, in Ref. 32. A similar branch is characteristic for all liquids without exception, including ^{3}He (Ref. 56) and liquid metals. The results of our studies show that this collective branch of excitations (os) markedly widens and is damped out when a certain value of the wave vector $q \sim (0.4–0.65)$ Å^{-1} is reached. We note that this damping of zero sound is characteristic of all van der Waals liquids, in which zero sound is not observed as a well defined mode at wave vectors above (0.8–1.0) Å^{-1}.

The *wide component* (w) is characteristic of both phases of liquid ^{4}He. At the present time there are different ideas about the physical interpretation of the wide component.

First let us discuss the interpretation of Priezzhev, based on comparison of the dispersion curves of the excitations in quantum and classical liquids. Experiments on neutron scattering in metals, liquid hydrogen, and other liquids in some range of inverse momenta give dispersion curves similar to the Landau curve in liquid ^{4}He but with much larger width. The presence of such branches can be related to the quasicrystalline nature of liquids of relatively short-wavelength excitations with wavelengths of the order of the interatomic spacing up to several coordination spheres. Liquid ^{4}He, which is primarily a quantum liquid, preserves some of the properties of a classical liquid. In the simplest approach based on the variational principle, the phonon–roton dispersion curve $\varepsilon(q)$ is related to the structure factor $S(q)$ as

$$\varepsilon(q) = \hbar^2 q^2 / 2MS(q).$$

The well known Feynman argument about identical particles shows that at small q and $T=0$ phonon excitations with wave function

$$\Psi = \left[\sum_s \exp(iqr_s) \right] \Phi \tag{2.9}$$

are the only possible excitations of a liquid. The picture is changed at finite temperatures as q increases up to a value of the order of the inverse particle separation. The small vibrational motions of the atoms in the harmonic wave and the diffusion motion of the individual atoms become of the same order of magnitude. As before, a wave function of the form (2.9) satisfies the variational principle, but now its uniqueness cannot be derived by using the same arguments as at small q. Therefore, we can (and must) assume the existence of wave functions of a different type corresponding to the "normal" state of the liquid. These wave functions must reflect the quasicrystalline nature of the motion of the helium atoms and must be localized near slowly diffusing centers, the motion of which is described by classical variables. The collective excitations of this "normal" component correspond to quasicrystal phonons in classical liquids. The large

width of these excitations is related to the smallness of the number of quasicrystal coordination spheres or the smallness of the coherence length.

Here we should note that the relative contribution of the intensities of the narrow (n) and wide (w) peaks can be regarded as yet another experimentally measurable long-range order parameter, the temperature dependence of which qualitatively resembles that of traditional order parameters like the density of the Bose condensate and the density of the superfluid component.

A different treatment of the two-branch structure of liquid ^{4}He has been given by Yarunin.[57] Just as the n component is associated with the presence of the Bose condensate, the w component is associated with the presence of atoms of momentum $p=0$, which are present in the superfluid and normal phases of liquid ^{4}He. The difference between them is that in the first case the atoms of the Bose condensate are located in the equilibrium position at the minimum of the potential curve, while in the second the atoms with momentum $p=0$ are excited from states outside the minimum.

An attempt to attribute the w component to neutron scattering on thermally excited quasiparticles encounters a difficulty. In this approach, as the temperature is decreased the intensity of the w component must tend to zero, owing to the decreased number of quasiparticles in the liquid. In our case (see Figs. 12 and 13) the w component is observed even at very low temperatures.

The *wide component* (r), whose maximum is located at energies above the spectrum of single-particle excitations $\varepsilon > 1.2$ meV, is observed in both phases of liquid ^{4}He. It has a strong temperature dependence; as T decreases the intensity of the r component falls to zero by definition. This scattering mode is associated with neutron scattering on thermally excited quasiparticles. The theory of such excitations is well developed for liquid Fermi systems[37] and has been used to interpret the data[56] on neutron scattering in liquid ^{3}He. The generalization to Bose systems is given in Refs. 38 and 39. Such processes are interpreted physically as the transfer of the energy of the scattered neutrons to thermally excited quasiparticles (phonons, maxons, rotons) already present in the system. The energy spectrum of such excitations is fundamentally different in that, instead of a dispersion curve corresponding to a line in $\varepsilon - q$ coordinates, there is a wide band or continuum, with a definite range of ε corresponding to each value of q. Therefore, the peaks in neutron scattering associated with these excitations must be very wide. This neutron scattering mechanism is always associated with density fluctuations of the medium and must be observed in both phases of ^{4}He. The intensity of excitations of this type must fall off rapidly with decreasing temperature, because the number of thermally excited quasiparticles in the liquid is significantly decreased. In general, this process can be attributed to multiphonon scattering of neutrons or, more precisely, to two-phonon scattering, because a neutron is scattered on an excitation present in the liquid and creates a single new excitation in the scattering. However, it should be added that in the maxon region of wave vectors the maximum of this wide peak is located at energies of order (2–3) meV. This might be explained by the fact that, in addition to the process discussed above, the simultaneous emission of two, three, or more excitations can occur in scattering on thermally excited quasiparticles.

The *wide component* (mf), which is weakly temperature-dependent, is also observed in both phases of liquid ^{4}He. As the temperature of liquid ^{4}He decreases, the intensity of the r component falls and the picture of this scattering component becomes clearer. Peaks appear in the mf spectrum. According to Ref. 34, they are associated with the emission of two, three, or more quasiparticles in neutron scattering. The mf component is attributed to multiphonon scattering of neutrons.

3. THE SEARCH FOR AND STUDY OF THE BOSE CONDENSATE IN LIQUID ^{4}He

Although the relation between the superfluidity of He II and the presence of a Bose condensate is indirect,[58] for a long time now it has been assumed that below the temperature of the λ point in liquid ^{4}He there is a Bose condensate of atoms with zero momentum.[59,60] This assumption is based primarily on the analogy with a nonideal Bose gas, but so far there is no completely rigorous proof of this assertion.[58] During the last half-century many experiments have been performed to look for the Bose condensate in superfluid ^{4}He. In addition, these experiments were able to confirm or reject an indirect relation between superfluidity and the presence of a Bose condensate.

Let us consider the most important ideas behind the search for a Bose condensate in superfluid ^{4}He and their implementation. We shall arbitrarily group some of them together.

In 1950 Goldstein *et al.*[61] suggested that the effect of Bose–Einstein statistics might be visible in neutron scattering by liquid ^{4}He. This can be regarded as the first attempt to construct a theory of the scattering of slow neutrons by liquid helium. Studying the inelastic scattering of neutrons with energy much larger than the value of k_BT of the liquid, they found that in passing through the λ point the scattering cross section at small angles is decreased, owing to the Bose condensation of some of the atoms. In addition, a decrease of the cross section associated with the impossibility of neutron heating on the atoms of a Bose condensate should be observed in the neutron-heating spectrum. However, the experiments performed at Los Alamos[62] and Harwell[63] did not find the expected change in the neutron scattering intensity in passing through the λ point.

Most experiments have been performed under conditions in which high-energy neutron scattering is characterized as one-atom scattering.[64–66] It was assumed that the measured dynamical structure factor splits into two terms, one of which pertains to scattering on the atoms of the Bose condensate, and the other to scattering on the atoms above the condensate. Measurements carried out at large wave vectors up to $q=23$ Å^{-1} (Refs. 71–74) showed that the Bose-condensate peak could not be distinguished, because it is widened by the final-state interaction.[71,75,76] Therefore, various mathematical models were used to describe the neutron-scattering spectra. These models allowed the density of the Bose condensate in liquid ^{4}He to be estimated. Experiments

were performed at various temperatures in order to obtain more reliable results. The estimates of the density of the Bose condensate at $T=0$ lie in the range $n_0/n\sim(0-14)\%$.

The studies to determine the density of the Bose condensate from the pair correlation function $g(r)$, obtained by measuring the static structure factor $S(q)$ in the liquid, should be mentioned.[67–70] The pair correlation function $g(r)$ for liquid ^{4}He is a function of temperature because some of the atoms at temperature $T<T_0$ go into the Bose-condensate state. The spatial uncertainty for atoms with momentum $\hbar\mathbf{p}=0$ decreases the amplitude of oscillation of the function $g(r)$ about $g(r)=1$. Measurements of the temperature dependence of the density of the Bose condensate gave $n_0/n\sim14\%$ for $T=0$.

Exact expressions for the momentum distribution $n(p)$ of the atoms for $p\to0$ and temperatures $T\to0$ and $T>0$ were obtained in the theoretical studies of Gavoret and Nozières[27] and Reatto and Chester.[77,78] The density of the Bose condensate can be determined by checking these dependences experimentally. However, the experimental technique is not yet developed enough to permit such measurements to be made.

In Ref. 79 it was suggested that the density of the Bose condensate can be estimated by using a small admixture of ^{3}He, which, in addition to destroying the superfluid state, also destroys the Bose condensate. If the momentum distribution $n(p)$ in liquid ^{4}He for atoms with $p\neq0$ depends weakly on the small admixture of ^{3}He, then for $T<T_\lambda$ the entire difference in the shapes of the spectra of neutrons scattered on pure ^{4}He and on the mixture ^{4}He+^{3}He will be due to the presence of the Bose condensate. Such an estimate of n_0/n is valuable because this method is independent of assumptions about the form of the scattering law $S(q,\varepsilon)$. This method is complicated to implement because it requires a very intense neutron beam, owing to the large cross section for neutron capture on ^{3}He atoms.

Another suggestion is that of Ref. 80, in which a method of determining the density of the Bose condensate from data on the average kinetic energy per atom in the liquid is discussed.

The temperature dependence of the relative density of the Bose condensate in liquid ^{4}He has been studied at the Joint Institute for Nuclear Research in the region of one-atom excitations, using the method of neutron inelastic scattering at temperatures $T=(0.42-4.2)$ K. The spectra of neutrons scattered by liquid ^{4}He were analyzed by means of a mathematical model with one or two Gaussians. The experimental data were analyzed by using the regularized Gauss–Newton iteration process.[81] Let us discuss these experiments in more detail.

3.1. The experimental conditions

Experiments to study the density of the Bose condensate in liquid ^{4}He were performed by the neutron time-of-flight method at the DIN-1M spectrometer in the booster mode of operation of the IBR-30 reactor. The initial energy of the neutrons incident on the sample was about $E_0\sim190$ meV. The spectra of neutrons scattered by liquid ^{4}He were measured at three scattering angles $\theta=96.5°$, 109.5°, and 122.6°. The energies of the recoil nuclei for these angles are $\varepsilon_0\approx82$, 93, and 102 meV, and the wave-vector transfers are $q_0\approx12.6$, 13.4, and 14.1 Å^{-1}. The initial neutron energy and scattering angles were chosen so that in the studied region of energy and wave-vector transfers the scattering system behaves as a quasifree system, because it satisfies, on the one hand, the requirement that the energy of the collective excitations be small compared with the energy transferred to the neutron and, on the other, the requirement that the ratio of the energy transferred to the neutron and the excitation energy of the free helium atom be close to unity. In these experiments this ratio was 0.98 ± 0.02.

As the initial energy of the neutrons is increased, the effect of the final-state interaction diminishes and the theory becomes more accurate.[64,65] Here it is necessary to take into account the fact that the width of the instrumental line, which is proportional to $E_0^{3/2}$, grows more quickly than the Doppler width, which grows as $E_0^{1/2}$. In these experiments the ratio of the squared widths of the spectrometer resolution function and the Doppler broadening on ^{4}He atoms is of order 0.2. Therefore, when the initial energy is increased above 190 meV, the width of the one-atomic peak will to a large degree be determined by the resolution function of the apparatus, and analysis of the shape of the peak becomes impracticable. To obtain a more accurate shape of the spectrum of neutrons scattered by liquid ^{4}He, the measurements were performed with the maximum possible statistical accuracy. The integrated count at the peak of one-atomic excitations at various temperatures of the liquid was $(2-5)\times10^5$ pulses.

3.2. Description of the models for analysis

The first experiments to study the spectrum of one-atomic excitations of liquid ^{4}He using neutron inelastic scattering[49,82–84] showed that under the existing experimental conditions ($q\sim14$ Å^{-1}) it is impossible to implement the suggestion of Hohenberg and Platzman.[64] We note that in the later experiments[73] at $q=23$ Å^{-1} it was also impossible to isolate directly the Bose-condensate peak. Estimates show that this can probably be done for $q>100$ Å^{-1}. Therefore, the experimental data were analyzed by the method of mathematical decomposition of the spectrum of scattered neutrons into condensate and above-condensate parts.[65] To obtain more reliable results for the density of the Bose condensate in liquid ^{4}He, and also to establish a possible relation between the phenomena of Bose condensation and superfluidity, the temperature dependences of the parameters of the mathematical decomposition were studied, along with that of the relative density of the Bose condensate.[49,85–92]

In the analysis, the experimental spectrum of neutrons scattered by liquid ^{4}He was described by two Gaussians according to the theory of Puff and Tenn[65] with the non-Gaussian correction proposed in Refs. 85 and 86:

$$\varphi(t)=E^2A_1\exp(P_1)+E^2A_4\exp(P_2)+(A_7+A_8\cdot t),$$

$$P_1=-(\varepsilon-\varepsilon_0+A_3)^2/A_2\cdot q^2;$$

$$P_2=-(\varepsilon-\varepsilon_0+A_6)^2/A_5\cdot q^2, \qquad (3.1)$$

where A_1-A_8 are free parameters, and t is the number of the time channel or the neutron time of flight. The first Gaussian describes neutron scattering on the atoms above the condensate, and the second describes scattering on the Bose condensate. The third term is introduced because the two-Gaussian model does not completely describe the experimentally observed spectrum at large energy transfers. This asymmetry of the one-atomic peak has also been observed in other experiments. Initially, attempts were made to attribute the larger intensity at the high-energy side to the presence in $n(p)$ at large momenta of either a maximum or a monotonically decreasing part of the spectrum.[93–95] Now the asymmetry of the one-atomic peak is associated with the final-state interaction, which leads to the appearance of an additive term in $S(q,\varepsilon)$. The separation of the dynamical structure factor into symmetric and asymmetric parts $S(q,\varepsilon)=S_s(q,\varepsilon)+S_a(q,\varepsilon)$ is discussed in Refs. 36, 71, and 94, where $S_a(q,\varepsilon)\to 0$ as the wave vector increases, and the symmetric part comes closer and closer to satisfying the impulse approximation (IA) $S_s(q,\varepsilon)\to S_{\mathrm{IA}}(q,\varepsilon)$. In our case the third term is partly related to neutron multiple scattering.

As the wave vector increases, the width of the Gaussian curve for the above-condensate atoms ($A_2^{1/2}$) increases as q, as in Doppler broadening, so that the factor q^2 is introduced for the parameter A_2. The introduction of the q^2 dependence for the condensate part can be explained by the fact that the final-state interaction is also proportional to q^2 (Ref. 65), if it is assumed that the total cross section for ^{4}He–^{4}He scattering is a weakly varying function in this range of q. The factor E^2 arises in going from the scattering law $S(q,\varepsilon)$ to the time spectrum of neutron scattering. The shifts A_3 and A_6 of the Gaussians relative to the excitation energy of the free helium atom reflect the fact that the helium atoms are located in a liquid and are quasifree.

All the experimental data were also analyzed without the Bose-condensate term ($A_4=0$), i.e., using the one-Gaussian model

$$\varphi(t)=E^2A_1\exp(P_1)+(A_7+A_8\cdot t). \tag{3.2}$$

The free parameters in (3.1) and (3.2) are the amplitudes of the Gaussian curves A_1 and A_4, the squared widths A_2 and A_5, the shifts A_3 and A_6 (in the calculations we generally set $A_3=A_6$), and the parameters A_7 and A_8. The statistical errors of the parameters were calculated according to error theory by the least-squares method.[96] The relative density of the Bose condensate was defined as the ratio

$$\xi=n_0/n=\varphi(n_0)/[\varphi(n_0)+\varphi(n_1)],$$

where $\varphi(n_0)$ and $\varphi(n_1)$ are the areas of the spectra for the condensate and above-condensate parts, respectively. The program COMPIL, JINR S-401, Dubna[81] was used to analyze the experimental data.

3.3. Analysis of the experimental data

The numerical analysis of the experimental data on the basis of the dependences (3.1) and (3.2) reduces to solving a nonlinear system of equations for various values of t for the unknowns A_1-A_8, with $A_3=A_6$. The number of unknowns

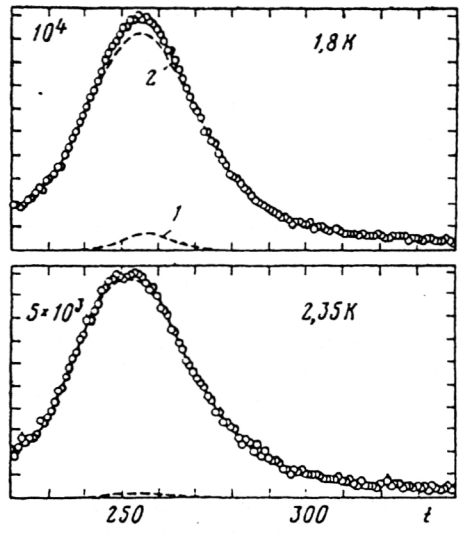

FIG. 25. Experimental spectra of neutrons scattered on liquid ^{4}He at $q=13.4$ Å^{-1} for $T=1.8$ and 2.35 K. The calculated curves pertaining to the Bose-condensate (curve 1) and above-condensate (curve 2) parts are shown by the dashed line.

was taken to be $m_1=5$ and $m_2=7$ for the one- and two-Gaussian models, respectively. In the solution we used statistical weights of the form $1/\sigma_t^2$, where σ_t is the standard deviation of the measured quantities and $t=1,2,\ldots,121$. This makes it possible to use the closeness of χ_i^2/s_i to unity as a statistical criterion for the quality of the approximations.[96] Here $i=1,2$ and $s_i=121-m_i$ is the number of degrees of freedom.

In Fig. 25 we show the experimental spectra of neutrons scattered by liquid ^{4}He at temperatures $T=1.8$ and 2.35 K for scattering angle $\theta=109.5°$. The dashed lines are the calculated curves pertaining to the condensate (curve 1) and above-condensate (curve 2) parts.

The width of the Gaussian curve for the condensate part is determined by the energy resolution of the spectrometer and the magnitude of the final-state interaction. In this case the calculated value of the squared width A_5 for the Bose-condensate Gaussian is mainly determined by the energy resolution of the spectrometer which, within several percent, is independent of the scattering angle and temperature and coincides with the corresponding resolution within the errors.

The values of the parameters A_3 and A_6 for the different measurements lie in the range (0–4) meV. On the basis of the calculations, it can be said that the energy transferred to a ^{4}He atom in the liquid in neutron scattering is about 2% smaller than the energy transferred to a free atom.

The width of the above-condensate part of the spectrum is determined by the thermal motion of the ^{4}He atoms or by the average kinetic energy per atom in the liquid (KE). The values of KE were calculated from the neutron spectrum described by the condensate and above-condensate Gaussians. In Fig. 26 we show the values of KE calculated by using the two-Gaussian model. For $T>T_\lambda$ the values of KE coincide for the two models within the errors, and for $T<T_\lambda$ the values of KE obtained from the one-Gaussian model are about 1

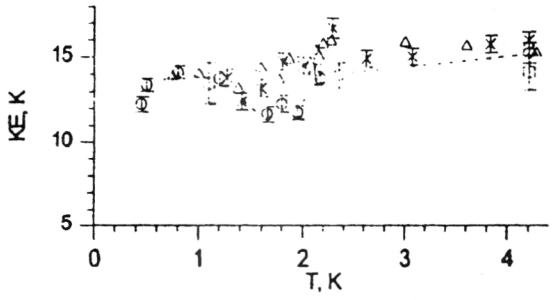

FIG. 26. Temperature dependence of the average kinetic energy per ^{4}He atom. The circles and dashed line are our data,[88,90] the triangles are the thermodynamical data,[80] the crosses are from Ref. 97, and the squares are from Ref. 98.

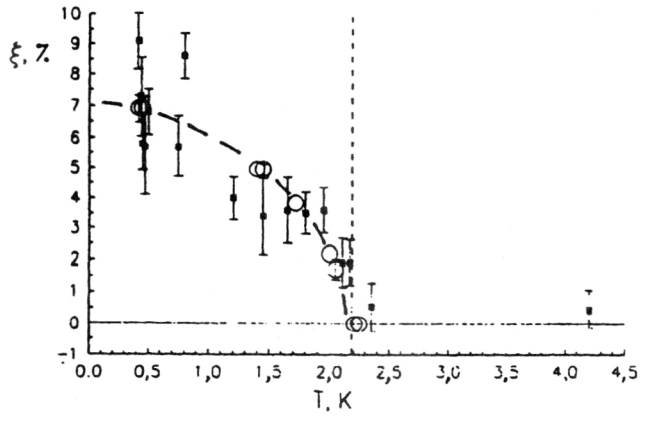

FIG. 27. Temperature dependence of the relative density of the Bose condensate in liquid ^{4}He. The dark squares are the results of the analysis of single-atom neutron scattering, and the light circles are the n component of the spectrum of single-particle excitations, normalized to n_0/n in the temperature range (0.4–0.5) K.

K lower. This is due to the fact that for $T>T_\lambda$ the two models give equally good descriptions of the experimental spectrum, while for $T<T_\lambda$ the neutron spectrum is described better by the two-Gaussian model. For comparison, in Fig. 26 we show the results for KE from Refs. 80, 97, and 98. These curves are similar to ours, but the values are slightly larger.

The analysis of the experimental data performed using the one-Gaussian and two-Gaussian models shows that the spectra of neutrons scattered by liquid ^{4}He are described satisfactorily. Complication of the two-Gaussian model by the addition of new Gaussians does not improve the description of the measured spectra. Comparison of the values of χ_1^2/s_1 for the one-Gaussian model and χ_2^2/s_2 for the two-Gaussian model shows that from the viewpoint of the statistical criterion, the experimental data obtained at temperatures $T>T_\lambda$ are described better by the one-Gaussian model, and for $T<T_\lambda$ by the two-Gaussian model. Let us consider the so-called dispersion ratio[99] $\mathscr{V}^2=(\chi_1^2/s_1)/(\chi_2^2/s_2)$, which characterizes the relative probability with which the models can be accepted or rejected. For $T>T_\lambda$ the dispersion ratio is $\mathscr{V}^2=0.99-1.01$. For $T<T_\lambda$ the dispersion ratio increases rapidly with decreasing temperature, and for $T\leqslant 1.8$ K it becomes greater than 1.2. Using the tabulated values of $\mathscr{V}^2$ from Ref. 99, for $s_1=116$ and $s_2=114$ we find that the significance criterion for accepting the two-Gaussian model for $T<T_\lambda$ is $f>80\%$, while for accepting the one-Gaussian model it is $f<20\%$. Meanwhile, for temperatures $T>T_\lambda$ the significance criteria for accepting these two models are about equal: $f=50\%$.

3.4. Temperature dependence of the relative density of the Bose condensate in liquid ^{4}He

The results of analyzing the experimental data to determine the relative density of the Bose condensate in liquid ^{4}He in the temperature range $T=(0.42-4.2)$ K are shown in Fig. 27. The temperature dependence of n_0/n has a singularity at temperature $T\approx T_\lambda$. For $T<T_\lambda$ the amount of Bose condensate is observed to increase with decreasing T. For $T>T_\lambda$ the value of the condensate density remains constant within the statistical error, so that this quantity can be assumed to be the systematic error associated with the experimental technique that was used and with the method of two-Gaussian decomposition of the neutron spectra. The level of the systematic error can be estimated by averaging the results of the calculation of the relative condensate density for $T>T_\lambda$ ($\sim 0.5\%$).

The calculated values of the relative density of the Bose condensate at temperatures $T<T_\lambda$ were described by the empirical formula

$$\xi=\xi_0[1-(T/T_0)^m],$$

where ξ_0 is the relative density of the Bose condensate for $T=0$, and T_0 is the Bose-condensation temperature. The values of the free parameters ξ_0, T_0, and m were determined by the method of least squares:

$$\xi_0=(7\pm 0.5)\%; \quad T_0=(2.22\pm 0.05)\ \text{K}; \quad m=3\pm 0.7.$$

This analysis reveals the temperature dependence of the density of the Bose condensate. The Bose condensate is observed for $T<T_0$, and it is not observed for $T>T_0$ within the accuracy of the experiment and the mathematical processing of the spectra. Within the errors, the Bose-condensation temperature coincides with the temperature of the transition of liquid ^{4}He to the superfluid state, $T_0\cong T_\lambda$. The temperature dependence of the Bose-condensate density is similar in nature to the temperature dependence of the measured density of the superfluid component in liquid ^{4}He (Ref. 100). Above the λ point there is no Bose condensate. It appears at the λ point and grows rapidly as the temperature is lowered.

It is interesting to look at the estimates of the maximum density of the Bose condensate at $T=1.2$ K obtained in the late 1960s. Let us assume that at the temperature $T=4.2$ K the density of the Bose condensate is zero, and the change in the shape of the spectrum of neutrons scattered by liquid ^{4}He as the temperature is decreased from 4.2 K to 1.2 K is entirely due to the condensation of ^{4}He atoms. Using the experimental spectra that we measured at wave vectors $q=(12-14)$ Å^{-1}, we find that the maximum amount of

Bose condensate in liquid ^{4}He at $T=1.2$ K is $\xi_{max}=(5.9\pm0.4)\%$. This result is in complete agreement with the data in Fig. 27.

For comparison, let us give the results for the density of the Bose condensate obtained recently in the measurements of Refs. 71–74. The temperature dependence of the relative density of the Bose condensate found in those studies is similar to that measured by us earlier. The authors of those studies obtained $n_0/n\cong 9\%$ for the density of the Bose condensate at $T=0$ K. Although this is rather close to our value, there is still a difference in the magnitude of the density.

CONCLUSION

Let us list the main results of the studies of liquid ^{4}He by the method of neutron inelastic scattering at the IBR-30 and IBR-2 reactors using the DIN-1M and DIN-2PI spectrometers. These studies were carried out for a wide range of energy transfers $\varepsilon\approx(0.1-200)$ meV, wave-vector transfers $q\approx(0.08-14)$ Å^{-1}, and temperatures $T=(0.42-4.2)$ K.

1. We have measured the structure of the excitation spectrum in liquid ^{4}He.

• The excitation spectrum in the phonon–maxon–roton region has a complicated structure depending on wave vector and temperature. The *decomposition of the sharp peak* in neutron scattering into several components with completely different dependences $\varepsilon(T)$, $Z(T)$, and $W(T)$ is a *new result*. Two excitation branches are seen in the normal phase of liquid ^{4}He. One of them (w) is observed throughout the region of studied wave vectors q and is characterized by large width of the peaks. The second branch (os) is clearly visible only at small q. These two branches are also characteristic of superfluid ^{4}He. For $T<T_\lambda$ a new component (n) is added to the structure of the dispersion curves in He I. This component is not observed above the phase-transition point. The intensity of this branch for $q>0.65$ Å^{-1} increases sharply with decreasing temperature and becomes dominant at low T.

• A positive anomalous dispersion is observed for all three components (n, os, and w) of the excitations in the phonon region of the spectrum. It becomes especially noticeable for the w component as T increases. As q decreases the dispersion curves of all three components approach each other.

• The dispersion curve for the w component appears to be slightly shifted, as it were, squeezed into the region of smaller wave vectors compared with the dispersion curve for the n component. Thus, the maxon maximum and roton minimum are observed at smaller q for the w component than for the n component.

• The dependence of the static structure factor on the wave vector in the phonon region at temperatures $T=(0.42-2.21)$ K was measured. It was found that as the temperature is raised below the λ point, the fairly smooth departure from the straight line obtained by Feynman and Pitaevskiĭ is replaced by a sharp jump near T_λ.

• In liquid ^{4}He a singularity on the dispersion curve was discovered in going from the phonon to the maxon region at $q\sim(0.5-0.65)$ Å^{-1}. Here the os component is damped out rapidly. The wide component (w) has singularities in the dependences $\varepsilon_w(q)$, $W_w(q)$, and $Z_w(q)$. The narrow component (n) seems to merge with the os component. In this range of q the anomaly of the dispersion curve vanishes, i.e., the dispersion curve intersects the line of first-sound speed. The singularity on the dispersion curve at $q\sim(0.5-0.65)$ Å^{-1} can be attributed, according to the theory of Iordanskiĭ and Pitaevskiĭ, to the decay of excitations into phonons. This is probably a case where the decay of excitations into phonons is observed independently of the processes associated with interactions between excitations.

• The temperature dependence of the lifetime of the n and w excitations in the maxon region was measured. Comparison with the dependence calculated using the roton theory of Landau and Khalatnikov showed that for $T<1.7$ K the calculated and experimental curves coincide for the n component, and as the λ point is approached they coincide for the w component.

• Analysis of the neutron heating and cooling spectra for liquid ^{4}He showed that the values of the temperatures obtained by using the detailed-balance equation coincided with those measured with a thermocouple.

• The experimentally measured relative contribution of the intensities of the narrow (n) and wide (w) components can be taken as yet another long-range order parameter, whose temperature dependence qualitatively resembles that of the traditional order parameters: the density of the Bose condensate and the density of the superfluid component.

2. A new technique was used to study the structure of the excitation spectrum in liquid ^{4}He. Its main feature is the use of neutrons with very low initial energy, below the energy of the multiphonon excitations. This led to improvement of the resolution function and suppression of multiphonon scattering processes. In this way the ground was prepared for analyzing the shape of the *sharp* peak in neutron scattering.

3. The temperature dependence of the relative density of the Bose condensate was measured in the range $T=(0.42-4.2)$ K by two independent and different methods.

• The density of the Bose condensate was obtained by analyzing the spectra of one-atom neutron scattering at energy transfers $\varepsilon\approx 100$ meV and wave-vector transfers $q\approx 14$ Å^{-1}.

• The temperature dependence of the integrated intensity of the n component was measured. Theoretically, it is proportional to the density of the Bose condensate.

• Analysis of the experimental data showed that the relative density of the Bose condensate in liquid ^{4}He at $T=0$ K is $n_0/n=(7\pm0.5)\%$.

• The Bose-condensation temperature coincides within the errors with the temperature of the transition of liquid ^{4}He to the superfluid state, $T_0=T_\lambda$.

• It can be stated that the temperature dependence of the relative density of the Bose condensate is similar in nature to the temperature dependence of the density of the superfluid component. Above T_λ there is no Bose condensate, within the errors; it appears at the λ point and grows rapidly with decreasing temperature.

I am happy to have the opportunity of thanking V. L. Aksenov, A. M. Balagurov, V. V. Golikov, L. P. Pitaevskiĭ, and F. L. Shapiro (deceased) for their interest in and useful

discussions about this work, and also L. Aleksandrov, I. V. Bogoyavlenskiĭ, V. A. Zagrebnov, L. V. Karnatsevich, V. G. Kolobrodov, V. A. Parfenov (deceased), V. B. Priezzhev, A. V. Puchkov, and V. S. Yarunin for their collaboration.

[1] P. L. Kapitza, Nature **141**, 74 (1938).
[2] L. D. Landau, Zh. Éksp. Teor. Fiz. **11**, 592 (1941) [in Russian]; J. Phys. USSR **11**, 91 (1947).
[3] F. London, Nature **141**, 643 (1938).
[4] N. N. Bogolyubov, Izv. Akad. Nauk SSSR, Ser. Fiz. **11**, 77 (1947) [in Russian].
[5] S. T. Belyaev, Zh. Éksp. Teor. Fiz. **34**, 417 (1958) [Sov. Phys. JETP **7**, 289 (1958)]; **34**, 433 (1958) [7, 299 (1958)].
[6] D. Henshaw and A. D. B. Woods, Phys. Rev. **121**, 1266 (1961).
[7] R. A. Cowley and A. D. B. Woods, Can. J. Phys. **49**, 177 (1971).
[8] E. C. Svensson, V. F. Sears, A. D. B. Woods, and P. Martel, Phys. Rev. B **21**, 3638 (1979).
[9] O. W. Dietrich, E. H. Graf, C. H. Huang, and L. Passell, Phys. Rev. A **5**, 1377 (1972).
[10] F. Mezei, Phys. Rev. Lett. **44**, 1601 (1980).
[11] A. D. B. Woods and E. C. Svensson, Phys. Rev. Lett. **41**, 974 (1978).
[12] L. Van Hove, Phys. Rev. **95**, 249 (1954).
[13] V. G. Liforov, M. N. Nikolaev, A. G. Novikov *et al.*, in *Proc. of the Conf. on Research Applications of Nuclear Pulsed Systems*, Vienna, 1966.
[14] V. G. Liforov, V. Z. Nozik, V. A. Parfenov, and V. A. Semenov, Preprint FÉI-140, Physics and Power Institute, Obninsk (1968) [in Russian].
[15] A. V. Abramov *et al.*, At. Energ. **66**, 316 (1989) [Sov. J. At. Energy].
[16] I. V. Bogoyavlenskiĭ, Yu. Yu. Milenko, L. V. Karnatsevich *et al.*, Cryogenics **3**, 498 (1983).
[17] I. Waller and P. Q. Froman, Ark. Fys. **4**, 183 (1952).
[18] Yu. Yu. Glazkov, Yu. V. Lisichkin, and V. A. Parfenov, in *Proc. of the Third All-Union Conf. on Neutron Physics* [in Russian], Kiev, 1975; *Neutron Physics* [in Russian], 1976, Chap. 2, p. 76.
[19] V. A. Ermakov, Zh. A. Kozlov, and M. L. Chelnokov, Report 3-89-479, JINR, Dubna (1989) [in Russian].
[20] A. Bijl, Physica **7**, 869 (1940).
[21] R. P. Feynman, Phys. Rev. **94**, 262 (1954).
[22] L. P. Pitaevskiĭ, Zh. Éksp. Teor. Fiz. **31**, 536 (1956) [Sov. Phys. JETP **4**, 439 (1957)].
[23] S. V. Iordanskiĭ and L. P. Pitaevskiĭ, Zh. Éksp. Teor. Fiz. **76**, 769 (1979) [Sov. Phys. JETP **49**, 386 (1979)].
[24] L. D. Landau and I. M. Khalatnikov, Zh. Éksp. Teor. Fiz. **19**, 637 (1949) [in Russian]; I. M. Khalatnikov, *Theory of Superfluidity* [in Russian] (Fizmatgiz, Moscow, 1971).
[25] L. P. Pitaevskiĭ, Zh. Éksp. Teor. Fiz. **36**, 1168 (1959) [Sov. Phys. JETP **9**, 830 (1959)].
[26] N. Hogenholtz and D. Pines, Phys. Rev. **116**, 489 (1959).
[27] J. Gavoret and P. Nozières, Ann. Phys. (N.Y.) **28**, 349 (1964).
[28] P. C. Hohenberg and P. C. Martin, Ann. Phys. (N.Y.) **34**, 291 (1965).
[29] P. Szepfaluzy and I. Kondor, Ann. Phys. (N.Y.) **62**, 1 (1974).
[30] A. Griffin and T. H. Cheung, Phys. Rev. A **7**, 2086 (1973).
[31] A. Griffin, Can. J. Phys. **65**, 1357 (1987).
[32] W. G. Stirling and H. R. Glyde, Phys. Rev. B **41**, 4224 (1990).
[33] H. R. Glyde and A. Griffin, Phys. Rev. Lett. **65**, 1454 (1990).
[34] H. R. Glyde, Phys. Rev. B **45**, 7321 (1992).
[35] H. R. Glyde, J. Low Temp. Phys. **93**, 861 (1993).
[36] H. R. Glyde, *Excitations in Liquid and Solid Helium* (Clarendon Press, Oxford, 1994).
[37] D. Pines and P. Nozières, *Theory of Quantum Liquids* (Benjamin, New York, 1966) [Russ. transl., Mir, Moscow, 1967].
[38] A. Griffin and E. F. Talbot, Phys. Rev. B **24**, 5075 (1981).
[39] A. Griffin and E. F. Talbot, Phys. Rev. B **29**, 2531 (1984).
[40] W. G. Stirling and H. R. Glyde, Phys. Rev. B **41**, 4224 (1990).
[41] E. F. Talbot, H. R. Glyde, W. G. Stirling, and E. C. Svensson, Phys. Rev. B **38**, 11229 (1988).
[42] N. M. Blagoveshchenskiĭ, I. V. Bogoyavlenskiĭ, L. V. Karnatsevich *et al.*, Pis'ma Zh. Éksp. Teor. Fiz. **57**, 414 (1993) [JETP Lett. **57**, 428 (1993)]; Preprint R3-92-578, JINR, Dubna (1992) [in Russian].
[43] I. V. Bogoyavlenskiĭ, L. V. Karnatsevich, Zh. A. Kozlov *et al.*, Fiz. Nizk. Temp. **20**, 626 (1994) [Low Temp. Phys. **20**, 489 (1994)].
[44] N. M. Blagoveshchenskiĭ, I. V. Bogoyavlenskiĭ, L. V. Karnatsevich *et al.*, Phys. Rev. B **50**, 16550 (1994); Preprint R3-94-125, JINR, Dubna (1994) [in Russian].
[45] Zh. A. Kozlov, L. A. Siurakshina, and V. S. Yarunin, in *Proc. of the Third ESF Workshop: Network on Quantum Fluids and Solids*, April 1995, p. 179.
[46] E. Monousakis and V. R. Pandharipande, Phys. Rev. B **33**, 150 (1986).
[47] K. H. Andersen, W. G. Stirling, R. Scherm *et al.*, Physica B **180/181**, 851 (1992).
[48] D. J. Hughes and R. B. Schwartz, *Neutron Cross Section* (Brookhaven National Laboratory, New York, 1958).
[49] Zh. A. Kozlov, V. A. Parfenov, and B. Sidzhimov, Report R3-7519, JINR, Dubna (1973) [in Russian].
[50] F. Mezei, Phys. Rev. Lett. **44**, 1601 (1980).
[51] F. Mezei and W. G. Stirling, in *Proc. of the Seventy-Fifth Jubilee Conf. on Helium-4*, edited by J. G. M. Armitage (World Scientific, Singapore, 1983), p. 111.
[52] B. N. Esel'son, V. N. Grigor'ev, V. G. Ivantsov, and É. Ya. Rudavskiĭ, *Properties of Liquid and Solid Helium* [in Russian] (Izd. Standartov, Moscow, 1978).
[53] E. C. Svensson and V. F. Sears, Physica B **137**, 126 (1986).
[54] E. C. Svensson, P. Martel, and A. D. B. Woods, Phys. Lett. **57A**, 439 (1976).
[55] W. G. Stirling, in *Proc. of the Seventy-Fifth Jubilee Conf. on Helium-4*, edited by J. G. M. Armitage (World Scientific, Singapore, 1983), p. 109.
[56] R. Scherm, K. Guckelsberger, B. Fak *et al.*, Phys. Rev. Lett. **59**, 217 (1987).
[57] V. S. Yarunin, Teor. Mat. Fiz. **96**, 37 (1993) [Theor. Math. Phys. (USSR)]; Preprint E17-94-152, JINR, Dubna (1994); V. S. Yarunin and L. A. Siurakshina, Physica A **215**, 261 (1995).
[58] V. L. Ginzburg, Usp. Fiz. Nauk **97**, 601 (1969) [Sov. Phys. Usp. **12**, 241 (1969)].
[59] F. London, *Superfluids*, Vols. 1 and 2 (Wiley, New York, 1954).
[60] N. N. Bogolyubov, *Collected Works*, Vols. 2 and 3 [in Russian] (Naukova Dumka, Kiev, 1970).
[61] L. Goldstein, D. Sweeney, and M. Goldstein, Phys. Rev. **77**, 319 (1950).
[62] H. S. Sommers, Jr., J. G. Dash, and L. Goldstein, Phys. Rev. **97**, 855 (1955).
[63] P. A. Egelstaff and H. London, Proc. R. Soc. London, Ser. A **242**, 374 (1957).
[64] P. C. Hohenberg and P. M. Platzman, Phys. Rev. **152**, 198 (1966).
[65] R. Puff and J. Tenn, Phys. Rev. A **1**, 125 (1970).
[66] R. Puff, Phys. Rev. **137**, A406 (1965).
[67] G. J. Hyland, G. Rowlands, and F. W. Cummings, Phys. Lett. **31A**, 465 (1970); Phys. Kondens. Materie **12**, 90 (1970).
[68] G. J. Hyland and G. Rowlands, J. Low Temp. Phys. **7**, 271 (1972); Phys. Lett. **62A**, 154 (1977).
[69] H. N. Robkoff, D. A. Ewen, and R. B. Hallock, Phys. Rev. Lett. **43**, 2006 (1979).
[70] V. F. Sears and E. C. Svensson, Phys. Rev. Lett. **43**, 2009 (1979).
[71] R. N. Silver, Phys. Rev. B **37**, 3794 (1988).
[72] T. R. Sosnick, W. M. Snow, P. E. Sokol, and R. N. Silver, Europhys. Lett. **9**, 707 (1989).
[73] T. R. Sosnick, W. M. Snow, and P. E. Sokol, Phys. Rev. B **41**, 11185 (1994).
[74] P. E. Sokol, Neutron News **4**, 22 (1993).
[75] P. A. Whitlock and R. Panoff, Can. J. Phys. **65**, 1409 (1987).
[76] D. M. Ceperley and E. F. Pollock, Phys. Rev. Lett. **56**, 351 (1986).
[77] W. P. Francis, G. V. Chester, and L. Reatto, Phys. Rev. A **1**, 86 (1970).
[78] L. Reatto and G. V. Chester, Phys. Rev. **155**, 88 (1966).
[79] V. A. Zagrebnov and V. B. Priezzhev, Preprint R17-9634, JINR, Dubna, 1969 [in Russian].
[80] V. F. Sears, Phys. Rev. B **28**, 5109 (1983).
[81] L. Aleksandrov, Preprint 5-6821, JINR, Dubna (1972) [in Russian]; Preprints R5-7258, R5-7259, JINR, Dubna (1973) [in Russian].
[82] R. A. Cowley and A. D. B. Woods, Can. J. Phys. **49**, 177 (1971).
[83] O. Harling, Phys. Rev. Lett. **24**, 1046 (1970).
[84] H. A. Mook, R. Scherm, and M. K. Vilkinson, Phys. Rev. A **6**, 2268 (1972).
[85] Zh. A. Kozlov, L. Aleksandrov, V. A. Zagrebnov *et al.*, Preprint R4-7895, JINR, Dubna (1974) [in Russian].
[86] L. Aleksandrov, V. A. Zagrebnov, Zh. A. Kozlov *et al.*, Zh. Éksp. Teor. Fiz. **68**, 1825 (1975) [Sov. Phys. JETP **41**, 915 (1975)].
[87] E. B. Dokukin, Zh. A. Kozlov, V. A. Parfenov, and A. V. Puchkov, Pis'ma Zh. Éksp. Teor. Fiz. **23**, 497 (1976) [JETP Lett. **23**, 453 (1976)].
[88] E. B. Dokukin, Zh. A. Kozlov, V. A. Parfenov, and A. V. Puchkov, Zh. Éksp. Teor. Fiz. **75**, 2273 (1978) [Sov. Phys. JETP **48**, 1146 (1978)].

[89] N. M. Blagoveshchenskiĭ, E. B. Dokukin, Zh. A. Kozlov *et al.*, HT-21, 131 (1980) [in Russian].
[90] N. M. Blagoveshchenskiĭ, I. V. Bogoyavlenskiĭ, L. V. Karnatsevich *et al.*, Pis'ma Zh. Éksp. Teor. Fiz. **37**, 152 (1983) [JETP Lett. **37**, 184 (1983)].
[91] I. V. Bogoyavlenskiĭ, L. V. Karnatsevich, Zh. A. Kozlov, and A. V. Puchkov, Fiz. Nizk. Temp. **16**, 139 (1990) [Low Temp. Phys. **16**, 77 (1990)].
[92] I. V. Bogoyavlenskiĭ, L. V. Karnatsevich, Zh. A. Kozlov, and A. V. Puchkov, Physica B **176**, 152 (1992).
[93] W. McMillan, Phys. Rev. **138**, A442 (1965).
[94] P. Martel, E. C. Svensson, A. D. B. Woods *et al.*, J. Low. Temp. Phys. **23**, 285 (1976).
[95] M. H. Kalos, D. Levesque, and L. Verlet, Phys. Rev. A **9**, 2178 (1974).
[96] Yu. V. Linnik, *Method of Least Squares and Principles of the Theory of Observations* (Pergamon Press, Oxford, 1961) [Russ. original, Fizmatgiz, Moscow, 1962].
[97] A. G. Gibbs and O. K. Harling, Phys. Rev. A **7**, 1748 (1973).
[98] A. D. B. Woods and V. F. Sears, J. Phys. C **10**, L341 (1977).
[99] N. P. Klepikov and S. N. Sokolov, *Analysis and Planning of Experiments Using the Maximum Liklihood Method* [in Russian] (Nauka, Moscow, 1964).
[100] E. Andronikashvili, J. Phys. (USSR) **10**, 201 (1946) [in Russian].

Translated by Patricia A. Millard